AWARD NUMBER: W81XWH-20-1-0795

TITLE: Improving Tendon Repair via Sensory Nerve NGF-TrkA Signaling for Retention on Duty

PRINCIPAL INVESTIGATOR: Aaron W. James

CONTRACTING ORGANIZATION: Johns Hopkins University, Baltimore, MD

REPORT DATE: January 2024

TYPE OF REPORT: Final

PREPARED FOR: U.S. Army Medical Research and Development Command
Fort Detrick, Maryland 21702-5012

REPORT DOCUMENTATION PAGE

Form Approved
OMB No. 0704-0188

1. REPORT DATE	2. REPORT TYPE	3. DATES COVERED
January 2024	Final	30Sep2020-29Sep2023

4. TITLE AND SUBTITLE

Improving Tendon Repair via Sensory Nerve NGF-TrkA Signaling for Retention on Duty

5a. CONTRACT NUMBER
W81XWH-20-1-0795

5b. GRANT NUMBER

5c. PROGRAM ELEMENT NUMBER

6. AUTHOR(S)
Aaron W. James

E-Mail:

5d. PROJECT NUMBER

5e. TASK NUMBER

5f. WORK UNIT NUMBER

7. PERFORMING ORGANIZATION NAME(S) AND ADDRESS(ES)

Johns Hopkins University
3400 N Charles St.
Baltimore, MD 21218

8. PERFORMING ORGANIZATION REPORT NUMBER

9. SPONSORING / MONITORING AGENCY NAME(S) AND ADDRESS(ES)

U.S. Army Medical Research and Development Command
Fort Detrick, Maryland 21702-5012

10. SPONSOR/MONITOR'S ACRONYM(S)

11. SPONSOR/MONITOR'S REPORT NUMBER(S)

12. DISTRIBUTION / AVAILABILITY STATEMENT

Approved for Public Release; Distribution Unlimited

13. SUPPLEMENTARY NOTES

14. ABSTRACT

Major tendon injuries represent a significant source of morbidity for military trainees, combat casualties and military veterans. Tendonitis or other tendon injuries represents a significant source of delay in military training. For example, in one long-term observational study following 80,106 active-duty personnel for one year, 450 cases of Achilles tendonitis and 584 cases of patellar tendinopathy were identified91. Furthermore, once injured, a tendon is predisposed to further injury, which sets up the patient for risk of chronic pain, psychosocial distress, and future disability. Better understanding of the pathophysiology of tendon repair will lead to more efficacious treatment strategies. This would represent a high impact on both individual and socioeconomic levels, among military and civilian populations.

15. SUBJECT TERMS
Tendon Repair

16. SECURITY CLASSIFICATION OF:			17. LIMITATION OF ABSTRACT	18. NUMBER OF PAGES	19a. NAME OF RESPONSIBLE PERSON
a. REPORT	b. ABSTRACT	c. THIS PAGE			USAMRDC
Unclassified	Unclassified	Unclassified	Unclassified	29	19b. TELEPHONE NUMBER *(include area code)*

TABLE OF CONTENTS

1. INTRODUCTION

Nerve fibers terminate at the surfaces of tendons, such as the paratenon, and include nociceptive, mechanoceptive, and autonomic fibers[26]. The most familiar and best-understood function of sensory nerves is pain sensation, which is profoundly apparent following tendon injury. The central mediator of pain sensation is NGF (Nerve growth factor), which transmits nociceptive signals either by directly activating TrkA (Tropomyosin receptor kinase A) sensory neurons or through indirect mechanisms, which enhance the response of other nociceptive pathways[27]. In addition to pain sensation, a body of literature suggests an evolutionarily conserved role of nerves in tissue regeneration. For example, the regeneration of a starfish appendages, fish fins, amphibian limbs, and deer antlers are all critically dependent on concomitant axonal regeneration[28, 29]. The few studies conducted to date in rodents show that NGF is markedly upregulated acutely following tendon injury[30], and that supraphysiologic supply of NGF or Substance P (SP) induce tendon repair[31-34]. Clinical observations suggest the crucial importance of neural inputs for tendon repair, where individuals with spinal cord injury[36], sciatica[37], or diabetic neuropathy[38] exhibit tendon degeneration or tendon rupture. In new preliminary data, Achilles tenotomy in a mouse model induces *Ngf* transcription in vascular smooth muscle and other local cell types, promoting tendon re-innervation and subsequent fibroproliferative response within the injury site. Moreover, intact innervation is integral to the tendon repair process, as neurectomy or TrkA inhibition impede these phases in tendon repair. In aggregate, our preliminary data suggest a model in which TrkA-expressing sensory neurons terminating on the outer layers of the Achilles tendon respond after injury to positively regulate tendon repair.

2. KEYWORDS

Musculoskeletal injury, musculoskeletal repair, musculoskeletal regeneration, tendon injury, tendon repair, tendon regeneration, innervation, NGF, TrkA

3. ACCOMPLISHMENTS

What were the major goals of the project?

The project contains two aims:

Aim 1: *Determine the phenotypic consequences of TrkA inhibition on Achilles tendon repair*.

Aim 2: *Validate small molecule TrkA agonists to promote Achilles tendon repair*.

What was accomplished under these goals?

- Phenotypic consequences of TrkA inhibition on Achilles tendon repair

To characterize the neural response to tendon injury, we used a punch biopsy injury model of the mouse Achilles tendon. Whole mount immunostaining for β III-tubulin (TUBB3), combined with collagen imaging by second harmonic generation (SHG), showed TUBB3$^+$ peripheral nerve fibers coursing parallel to the tendon body and predominantly lying within the tendon sheath in the uninjured tendon (**Fig. 1A**). After injury, sprouting and disorganization of nerve fibers was identified surrounding the injury site (**Fig. 1B**). The temporal kinetics of peripheral nerve growth were further defined using sagittal sections of the Achilles tendon across a 42d period after injury (**Fig. 1C**). Relative staining for TUBB3$^+$ nerves increased significantly over uninjured control as early as 7d post-injury, peaked after 14d, and returned to baseline at d42 (**Fig. 1D,** $p<0.05$). In our previous reports in bone regeneration, peripheral nerves and blood vessels showed close temporospatial interactions. To investigate this phenomenon in the context of tendon repair, immunostaining for cluster of differentiation 31 (CD31), a marker for blood vessels, was evaluated in adjacent sections of those for TUBB3 (**Fig. 1, E and F**). Like TUBB3, CD31 was observed within the tendon sheath at baseline, followed by a rapid increase in injury site over the first 14d and returned to baseline after 42d (**Fig. 1F**, $p<0.05$). Cell proliferation was next assessed by marker of proliferation Ki-67 immunostaining on serial sections of the tendon injury site (**Fig. 1, G and H**). Temporal changes in the frequency of Ki67$^+$ cells mirrored those of neurovascularity of the injury site (**Fig. 1H**, $p<0.05$). The majority of peripheral nerves are NGF-responsive, TrkA-expressing neurons, therefore, changes in NGF expression were evaluated in a validated transgenic mouse model in which the NGF promoter controls the synthesis of enhanced green fluorescent protein (eGFP) (**Fig. 1, I and J**). The uninjured Achilles tendon had little eGFP reporter activity, however eGFP was increased by 7d post-injury indicating increased expression of NGF (**Fig. 1, I** and **K**, $p<0.01$). Immunofluorescent staining for TUBB3 showed peripheral nerves in the injury site within domains of NGF-eGFP reporter activity (**Fig. 1J**). Quantification of NGF reporter immunostaining indicated that the peak in NGF-eGFP expression was 7d post-injury (**Fig. 1K**, $p<0.01$). Finally, we assessed the cell types expressing the NGF reporter 7d after tendon injury (**Fig. 1, L and M**). As in other tissues, both eGFP$^+$ inflammatory and mesenchymal cells appeared to populate the tendon injury site, including broadly identified immune cells (CD45$^+$) and F4/80$^+$ macrophages (**Fig. 1L**), as well as mesenchymal cells expressing platelet-derived growth factor receptor α (PDGFRα), α smooth muscle actin (αSMA), and to a lesser extent tenomodulin (TNMD) (**Fig. 1M**), whereas CD31$^+$ endothelial cells (EC) were not observed to express eGFP (**not shown**). In summary, NGF expression in macrophage and mesenchymal cells of the tendon injury site is followed by transient tendon-associated nerve sprouting as well as vascular and proliferative changes in the cascade of tendon repair.

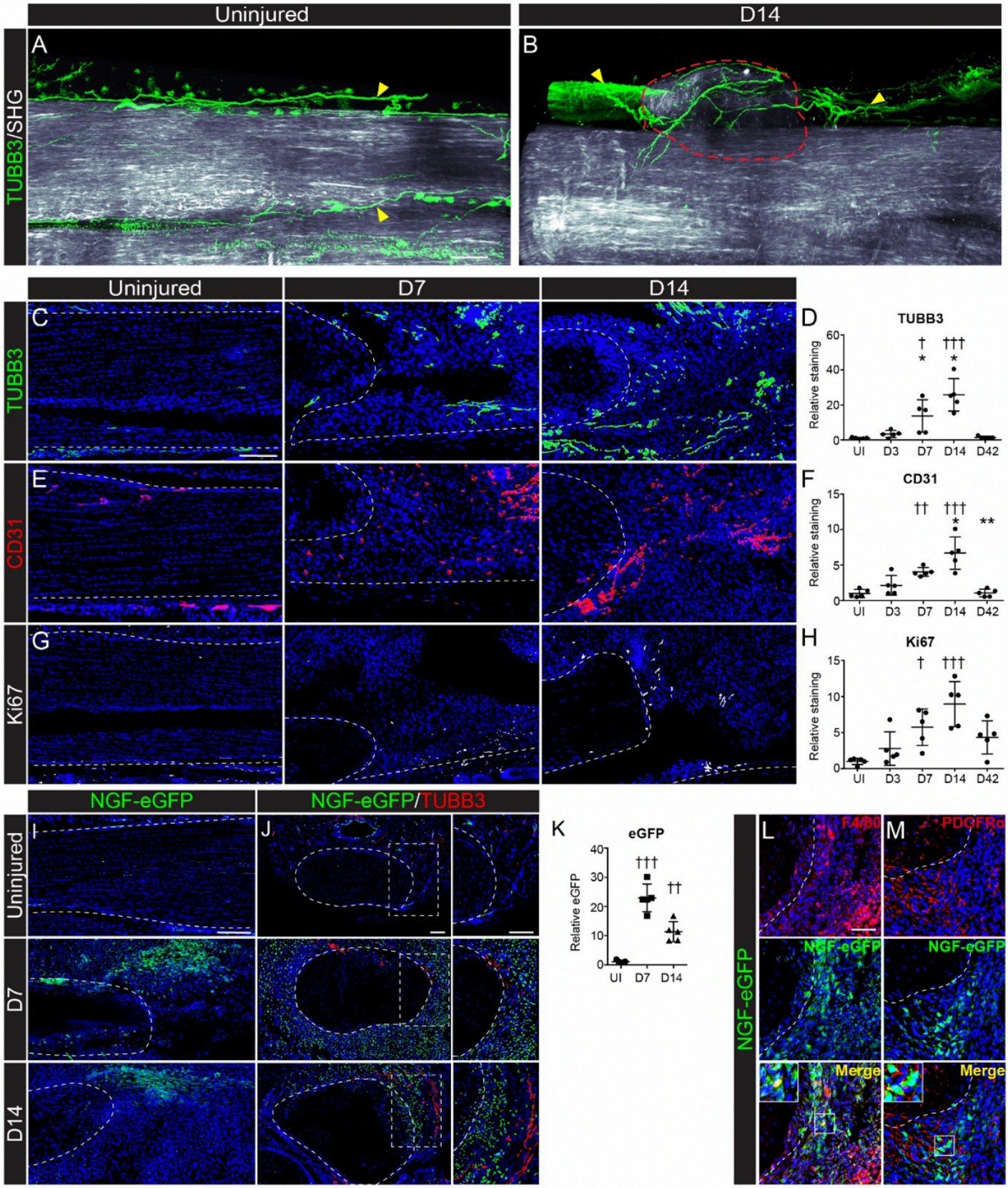

FIG. 1. NEUROVASCULAR INGROWTH IS AN EARLY RESPONSE TO MURINE ACHILLES TENDON INJURY. (**A and B**) Whole mount imaging of the murine Achilles tendon with second harmonic generation (SHG, grayscale) for tendon extracellular matrix and β III-tubulin (TUBB3) immunostaining (green). Yellow arrowheads indicate nerve fibers, red dashed line indicates injured area. (**C**) Representative TUBB3 immunofluorescent staining (green) in sagittal sections of the Achilles tendon before and after injury, additional images in **fig. S1**. (**D**) Quantification of relative staining of TUBB3 in uninjured (UI) and 3-42d post-injury. (**E**) Endothelial marker CD31 immunofluorescent staining (red) and (**F**) quantification of CD31 staining. (**G**) Proliferation marker Ki67 immunofluorescent staining (white) and (**H**) quantification of Ki67 staining. (**I**) NGF-eGFP reporter (green) in sagittal sections of the tendon before and after injury. (**J**) NGF-eGFP reporter (green) and TUBB3 immunofluorescent staining (red) on axial sections. (**K**) Quantification of NGF-eGFP reporter staining. (**L-Q**) Immunofluorescent staining for cell-specific markers on NGF-eGFP reporter

sections 7 d post-injury, including (**L**) F4/80 and (**M**) platelet derived growth factor receptor α (PDGFRα□. Green (NGF-eGFP), red (F4/80 or PDGFRα), and merged channels are shown separately. Nuclei are in blue and visualized with 4′,6-diamidino-2-phenylindole (DAPI) staining. Graphs show mean ± 1 SD, datapoints represent individual animal measurements. N=5 mice per timepoint. $^{\dagger}p<0.05$; $^{\dagger\dagger}p<0.01$; $^{\dagger\dagger}p<0.001$ in comparison to uninjured; $*p<0.05$; $**p<0.01$ in comparison to D7. One-way ANOVA with Tukey's post-hoc test. All scale bars: 100 μm. White dashed rectangles indicate areas of higher magnification. Curved dashed white lines indicate the margins of the Achilles tendon.

The majority of sensory neurons that innervate skeletal structures express the high affinity receptor for NGF, TrkA. In prior studies, we leveraged the availability of a previously characterized chemical-genetic approach to temporally inhibit TrkA catalytic activity by administration of a small molecule inhibitor in mice. $TrkA^{F592A}$ mice have a point mutation in exon 12 of the neurotrophic receptor tyrosine kinase 1 (*Ntrk1)* gene, allowing for TrkA kinase inhibition by the small molecule 1NMPP1 whereas $TrkA^{WT}$ mice are insensitive to 1NMPP1, and have no phenotypic changes in their Achilles tendon at baseline. Like *Ngf* conditional knockout animals, tendon healing, as determined by H&E staining and histologic scoring (**Fig. 2, A and B**) and enhanced μCT imaging (**Fig. 2, C and D**) was significantly reduced in 1NMPP1-treated $TrkA^{F592A}$ animals in comparison with age-matched, 1NMPP1-treated $TrkA^{WT}$ 14d following injury (**Fig. 2, A to D,** $p<0.05$). Immunofluorescent staining for neurovascularity of the injury site using axial sections of injured $TrkA^{WT}$ and $TrkA^{F592A}$ mice showed that TrkA inhibition led to a significant reduction of $TUBB3^{+}$ nerves (**Fig. 2, E and F**, $p<0.05$) and a reduction in $CD31^{+}$ ECs in the injured area (**Fig. 2, G and H**, $p<0.05$). Cell proliferation and tenocyte differentiation were assessed within the injured area of TrkA-inhibited animals by Ki67 and TNMD immunostaining, respectively (**Fig. 2, I to L**). $Ki67^{+}$ (**Fig. 2, I and J,** $p<0.05$) and $TNMD^{+}$ cells were significantly reduced in $TrkA^{F592A}$ tendon injuries relative to those in $TrkA^{WT}$ (**Fig. 2, K and L,** $p<0.05$). Thus, inhibition of TrkA kinase activity during tendon repair led to deficits in neo-innervation and regeneration.

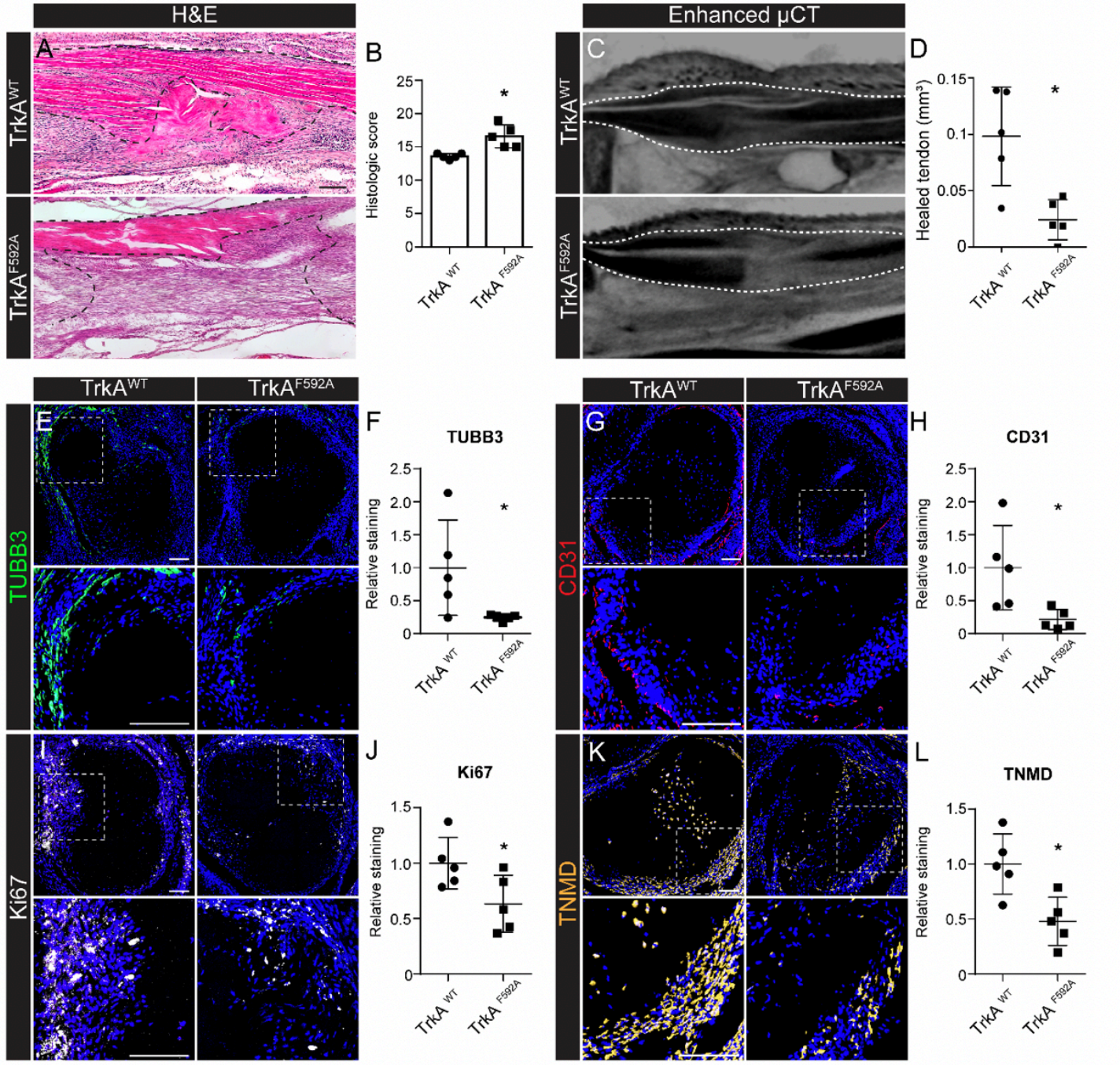

FIG. 2. TEMPORALLY CONTROLLED TRKA INHIBITION REDUCES TENDON NEUROVASCULARIZATION AND REPAIR. (**A**) H&E staining on sagittal sections of the injury site, black dashed lines indicate margins of tendon. (**B**) Histological score of healing in sagittal sections. (**C**) Enhanced µCT shown in sagittal cross-section, white dashed lines indicate margins of tendon. (**D**) µCT quantification of Achilles tendon volume within the injured area. (**E**) Innervation of the injury site in axial sections (TUBB3, green) and (**F**) relative staining quantification. (**G**) Vascularization of the injury site (CD31, red) and (**H**) relative staining quantification. (**I**) Cell proliferation of the injury site (Ki67, white) and (**J**) quantification. (**K**) Tenomodulin staining (TNMD, yellow) within axial sections of the tendon injury site and (**L**) relative staining quantification. Graphs show mean ± 1 SD, datapoints represent individual animal measurements. *p<0.05 in relation to TrkA^{WT} control using a two-tailed Student's t test. Scale bars: 100 µm. White dashed rectangles indicate areas of higher magnification. N=5 mice per genotype.

- Small molecule TrkA agonists to promote Achilles tendon repair

Having observed that genetic or surgical approaches to inhibit NGF, TrkA signaling, or sensory nerves impeded tendon repair, we next sought to encourage tendon neo-innervation and repair by boosting TrkA activation. A small molecule partial agonist of TrkA, gambogic amide (GA, 0.4 mg/kg i.p. daily over the repair period) was employed to test the effect of stimulating TrkA in tendon injury. H&E-stained sagittal sections demonstrated improved overall organization and improved healing score among GA-treated tendon injuries (**Fig. 3, A and B, fig. S18**). Enhanced µCT imaging confirmed these observations, showing a significant increase in healed tendon volume in the GA-treated group ($p<0.05$) (**Fig. 3, C and D**). As expected, TUBB3^{+} peripheral nerve fibers showed a

significant increase among GA-treated animals ($p<0.01$) (**Fig. 3, E and F**). Increased injury site innervation was accompanied by a significant increase in $CD31^+$ blood vessels in the GA-treated group ($p<0.05$) (**Fig. 3, G and H**). Improved healing metrics by TrkA partial agonism were accompanied by increases in cell proliferation and differentiation, as measured by Ki67 (**Fig. 3, I and J)** and TNMD immunostaining (**Fig. 3, K and L)**. A significant increase in both Ki67 and TNMD immunostaining was observed around the tendon body among GA-treated mice ($p<0.05$). Therefore, activation of TrkA signaling using a systemic small molecule has downstream effects of local tendon cell proliferation and differentiation, improving innervation, vascularization, and metrics of tendon healing.

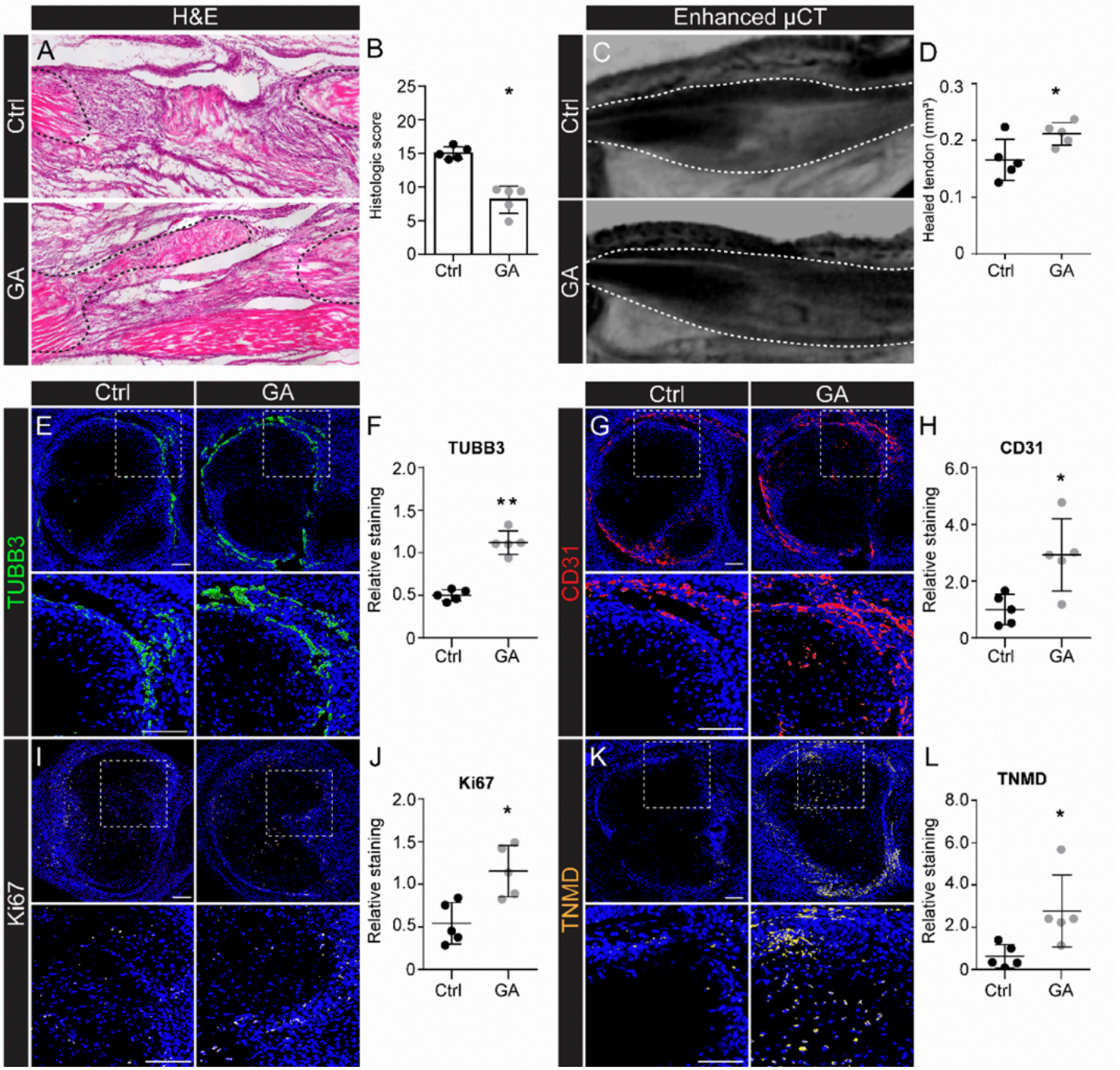

FIG. 3. TRKA AGONISM ENHANCES TENDON NEUROVASCULARIZATION AND REPAIR. C57BL/6J 12-wk-old (**A**) H&E staining performed on sagittal sections of the injury site. Dashed black lines indicate margins of tendon. (**B**) Histological score of healing (Modified Movin's score), as assessed using H&E-stained sagittal sections. Detailed breakdown of scoring by each parameter can be found in **fig. S17**. (**C**) Enhanced µCT imaging, shown in sagittal cross-section. (**D**) µCT quantification of Achilles tendon volume within the injured area. (**E**) Assessment of tendon site innervation, using β III-tubulin (TUBB3) immunofluorescent staining of axial sections. (**F**) Quantification of (E). (**G**) Assessment of tendon site vascularization, using CD31 immunofluorescent staining of axial sections. (**H**) Semi-quantitative analysis of (G). (**I**) Assessment of tendon site proliferation, using Ki67 immunofluorescent staining of axial sections. (**J**) Semi-quantitative analysis of (I). (**K**) Assessment of Tenomodulin (TNMD) immunofluorescent staining of axial sections. (**L**) Semi-quantitative analysis of (K). Graphs show mean ± 1 SD, datapoints represent individual animal measurements. *$p<0.05$; **$p<0.01$ in comparison to control group. Two-tailed Student's *t* test. Scale bar: 100 µm. White dashed rectangles indicate area of higher magnification. N=5 mice per group.

Key outcomes and conclusions:

Our work demonstrates that TrkA signaling plays a critical role in Achilles tendon repair in mice, and implicate peripheral nerves as important paracrine regulators of tissue repair in this context. Additional work which complements the funded work was performed, which was recently published in *Science Translational Medicine*. This included additional models such as transgenic animals which lack NGF expression in tendon injury site cells, mice exposed to surgical sural neurectomy to surgically ablate nerves, as well as reporter systems that differentiate tendon sheath progenitor cells from tenocytes. The published abstract from our Science Translational Medicine work is shown within Section 4 impact below, and the full manuscript is added to the appendix.

What opportunities for training and professional development has the project provided?

This project provided a number of opportunities for the postdoctoral participants to learn various techniques for mouse experiments, tendon injuries and analyses, as well as to acquire in-depth knowledge of signaling molecules and mechanisms involved in tendon regeneration.

How were the results disseminated to communities of interest?

Our novel findings have been disseminated by publication in scientific journals.

What do you plan to do during the next reporting period to accomplish the goals?

N/A

4. IMPACT

What was the impact on the development of the principal discipline(s) of the project?

The project supported our understanding of how peripheral neurons regulate the early stages of tendon repair. This project, in combination with additional work performed in parallel, culminated in a recent Science Translational Medicine publication. The abstract of this work is shown below, which summarizes overall impact of our work:

Peripheral neurons terminate at the surface of tendons partly to relay nociceptive pain signals, however, the role of peripheral nerves in the tendon injury-repair process beyond the afferent functions is not fully understood. Here, we showed that nerves sprout after Achilles tendon injury in domains of nerve growth factor (NGF) expressing cells in mice. Conditional deletion of *Ngf* in either myeloid or mesenchymal cell types limited both innervation and tendon repair. Similarly, inhibition of the NGF receptor tropomyosin receptor kinase A (TrkA) abrogated tendon healing. Sural nerve transection blocked the post-injury increase in tendon sensory innervation as well as blocking the expansion of tendon sheath progenitor cells (TSPCs) expressing tubulin polymerization promoting protein family member 3 (*Tppp3*). A combination of single cell and spatial transcriptomics revealed that disruption of sensory innervation caused dysregulated inflammatory and transforming growth factor β (TGFβ) signaling in tendon injuries. *In vitro* studies where dorsal root ganglia neuron conditioned media was supplemented to TSPCs further supported a role for neuronal mediators through TGFβ signaling in TSPC proliferation. Transcriptomic and histologic analyses of injured human tendons supported a role of innervation and TGFβ signaling in human tendon regeneration. Finally, systemic treatment with a small molecule partial agonist of TrkA after tendon injury increased neurovascular response, TGFβ signaling, TSPC expansion, and improved metrics of tissue repair. Although further studies will have to account for the potential effects of denervation on mechanical loading, we collectively provide evidence that peripheral innervation is critical for the regenerative response after acute tendon injury. Promoting neo-innervation might be a therapeutic means to speed tendon repair.

What was the impact on other disciplines?

Nothing to Report

What was the impact on technology transfer?

Nothing to Report

What was the impact on society beyond science and technology?

Nothing to Report

5. CHANGES/PROBLEMS

Changes in approach and reasons for change

Nothing to Report

Actual or anticipated problems or delays and actions or plans to resolve them

Nothing to Report

Changes that had a significant impact on expenditures

Nothing to Report

Significant changes in use or care of human subjects, vertebrate animals, biohazards, and/or select agents

Nothing to Report

6. PRODUCTS

- ### Publications, conference papers, and presentations

Journal publications.

1. Cherief M, Xu J, Li Z, Tower RJ, Ramesh S, Qin Q, Gomez-Salazar M, Yea JH, Lee S, Negri S, Xu M, Price T, Kendal AR, Fan CM, Clemens TL, Levi B, James AW. TrkA-mediated sensory innervation of injured mouse tendon supports tendon sheath progenitor cell expansion and tendon repair. Sci Transl Med. 2023 Dec;15(727):eade4619.

Books or other non-periodical, one-time publications.

Nothing to Report

Other publications, conference papers and presentations.

Nothing to Report

- ### Website(s) or other Internet site(s)

Nothing to Report

- ### Technologies or techniques

Nothing to Report

- ### Inventions, patent applications, and/or licenses

Nothing to Report

- ### Other Products

Nothing to Report

7. PARTICIPANTS & OTHER COLLABORATING ORGANIZATIONS

What individuals have worked on the project?

Name:	Aaron James
Project Role:	PI
Researcher Identifier	https://orcid.org/0000-0002-2002-622X
Nearest person month worked:	1.2
Contribution to Project:	Dr. James has overseen all aspects of the project.

Funding Support:	NIH, DoD, American Cancer Society, Maryland Stem Cell Research Fund, ALSF

Name:	Benjamin Levi, M.D
Project Role:	Co-I
Researcher Identifier	
Nearest person month worked:	.01
Contribution to Project:	Dr. Levi supervised surgical and in vivo studies in Aims 1 and 2.
Funding Support:	NIH, DoD

Name:	Mary Archer
Project Role:	Lab Manager
Researcher Identifier	
Nearest person month worked:	1
Contribution to Project:	Assist in tissue organization and analysis.
Funding Support:	NIH, DoD
Name:	Mingxin Xu
Project Role:	Postdoctoral Researcher
Researcher Identifier	
Nearest person month worked:	5.0
Contribution to Project:	Performed histology analysis.
Funding Support:	NIH, DoD

Name:	Alec Bancroft
Project Role:	Research Technician II
Researcher Identifier	
Nearest person month worked:	3
Contribution to Project:	Performed histology analysis.
Funding Support:	NIH

Name:	Pranathi Dasari
Project Role:	Lab Manager
Researcher Identifier	
Nearest person month worked:	0.6
Contribution to Project:	Prepared and processed of histology.
Funding Support:	NIH, DoD

Has there been a change in the active other support of the PD/PI(s) or senior/key personnel since the last reporting period?

Nothing to Report

What other organizations were involved as partners?

University of Texas, Southwestern
5323 Harry Hines Blvd
Dallas, TX 75390-9020

8. SPECIAL REPORTING REQUIREMENTS

COLLABORATIVE AWARDS:

Not applicable

QUAD CHARTS:

Improving tendon repair via sensory nerve NGF-TrkA signaling for retention on duty

OR190116
W81XWH-20-10795

PI: Aaron W. James, MD, PhD **Org:** Johns Hopkins University / UTSW **Award Amount:** $750,000

Study/Product Aim(s)

- Determine the phenotypic consequences of TrkA inhibition on Achilles tendon repair (Aim 1)
- Validate small molecule TrkA agonists to promote Achilles tendon repair (Aim 2)

Approach

Tendon overuse, tendonitis, and/or major tendon injuries, including rupture, occur at high rates during military training and in active duty military personnel. Our preliminary findings have led us to our overall hypothesis that NGF elicited by tendon injury induces TrkA$^+$ nerve ingrowth, which positively regulates tendon repair. Here, we examine the effects of TrkA agonism and antagonism on nerve ingrowth, tenocyte differentiation and tendon repair in an experimental mouse model of Achilles tendon injury.

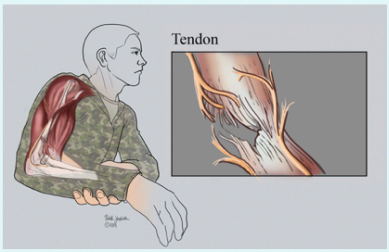

The proposed work examines the role of TrkA-expressing peripheral afferent neurons in the response to tendon injury, and the promotion of tendon repair in mice.

Accomplishment: Supported by the PRORP, we demonstrated the critical importance of TrkA+ neurons in regulating tendon repair and discovered potential neural-based therapeutics for tendon regeneration.

Timeline and Cost

Activities CY	21	22
Regulatory (Major task 1)		
TrkA inhibition (Major task 2)		
TrkA agonism (Major task 3)		
Estimated Budget ($K)	**$379**	**$371**

Updated: (1/20/2024)

Goals/Milestones
CY21 Goals –
x ACUC / ACURO approval and animal breeding
x Initiate TrkA inhibitor studies in mice
x Analyze effects of TrkA inhibition in mice
CY22 Goals –
x Finalize TrkA inhibitor experiments in mice
x Perform TrkA agonist experiments in mice
x. Complete TrkA agonist experiments in mice
Comments/Challenges/Issues/Concerns
- None.

Budget Expenditure to Date
Projected Expenditure: $750,000
Actual Expenditure: $748,391

9. APPENDICES:

- Award Expiration Transition Plan
- Publication in Science Translational Medicine

TENDINOPATHY

TrkA-mediated sensory innervation of injured mouse tendon supports tendon sheath progenitor cell expansion and tendon repair

Masnsen Cherief[1]†, Jiajia Xu[1]†, Zhao Li[1]†, Robert J. Tower[2], Sowmya Ramesh[1], Qizhi Qin[1], Mario Gomez-Salazar[1], Ji-Hye Yea[1], Seungyong Lee[1], Stefano Negri[1,3], Mingxin Xu[1], Theodore Price[4], Adrian R. Kendal[5], Chen-Ming Fan[6], Thomas L. Clemens[7,8], Benjamin Levi[2], Aaron W. James[1]†*

Peripheral neurons terminate at the surface of tendons partly to relay nociceptive pain signals; however, the role of peripheral nerves in tendon injury and repair remains unclear. Here, we show that after Achilles tendon injury in mice, there is new nerve growth near tendon cells that express nerve growth factor (NGF). Conditional deletion of the *Ngf* gene in either myeloid or mesenchymal mouse cells limited both innervation and tendon repair. Similarly, inhibition of the NGF receptor tropomyosin receptor kinase A (TrkA) abrogated tendon healing in mouse tendon injury. Sural nerve transection blocked the postinjury increase in tendon sensory innervation and the expansion of tendon sheath progenitor cells (TSPCs) expressing tubulin polymerization promoting protein family member 3. Single cell and spatial transcriptomics revealed that disruption of sensory innervation resulted in dysregulated inflammatory signaling and transforming growth factor–β (TGFβ) signaling in injured mouse tendon. Culture of mouse TSPCs with conditioned medium from dorsal root ganglia neuron further supported a role for neuronal mediators and TGFβ signaling in TSPC proliferation. Transcriptomic and histologic analyses of injured human tendon biopsy samples supported a role for innervation and TGFβ signaling in human tendon regeneration. Last, treating mice after tendon injury systemically with a small-molecule partial agonist of TrkA increased neurovascular response, TGFβ signaling, TSPC expansion, and tendon tissue repair. Although further studies should investigate the potential effects of denervation on mechanical loading of tendon, our results suggest that peripheral innervation is critical for the regenerative response after acute tendon injury.

INTRODUCTION

Pain is a clinical feature of tendon injury (*1*), and damaged tendons undergo poor healing, likely due to both intrinsic properties of the tendon and extrinsic tissue properties, such as neural and humoral response (*2*). Each year, there are approximately 17 million tendon and ligament injuries that require medical treatment in the United States alone, with an estimated economic cost of over $40 billion (*3*). Common clinical treatments such as anti-inflammatory medications (*4*), platelet-rich plasma (*5*–*7*), or physical therapy poorly address tendon healing (*8*). Peripheral neurons terminate at the surfaces of tendons (including the paratenon, endotenon, and epitenon) partly to relay nociceptive signals (*9*–*11*). The role of peripheral neurons in the tendon injury-repair process has been examined in previous studies (*9*–*11*); however, this remains an area in need of further study.

Recent studies from our laboratory have demonstrated an essential role for skeletal sensory nerves in healing of experimental injuries in adult mouse bone (*12*, *13*). In these experimental models, nerve growth factor (NGF), through its high-affinity receptor tropomyosin receptor kinase A (TrkA), induces skeletal reinnervation, which is essential for later cellular processes in bone repair, including revascularization and bone matrix deposition (*12*–*14*). Peripheral sensory nerves are also present on the surfaces of tendons (*11*), and clinical observations suggest an importance of neural inputs for tendon repair (*15*). For example, individuals with spinal cord injury (*16*), sciatica (*17*), or diabetic neuropathy (*18*) exhibit tendon degeneration or increased propensity for tendon rupture. To date, limited experimental studies in rodents have determined that supraphysiologic supply of NGF or neuropeptides aids tendon healing (*19*–*22*). The mechanisms underlying neural control of tendon repair are undetermined. Here, we show that NGF-responsive sensory nerves sprout after acute tendon injury in the paratenon to induce tendon sheath progenitor cell (TSPC) proliferation and injury site vascularization. A combination of single cell and spatial sequencing coupled with in vitro transcriptomics uncovered immunoregulatory and regenerative signals provided by injured nerves to orchestrate tendon healing. Results suggest that early ingrowth of $TrkA^+$ nerves regulates multiple cellular aspects of tendon repair, including mesenchymal, endothelial, and inflammatory cell behavior. The modulation of TrkA signaling may represent a potential therapeutic approach to enhancing tendon repair and improving proper tissue regeneration.

RESULTS

Peripheral nerves respond to Achilles tendon injury

To characterize the neural response to tendon injury, we used a punch biopsy injury model of the mouse Achilles tendon. Whole-mount

[1]Department of Pathology, Johns Hopkins University, Baltimore, MD 21205, USA. [2]Center for Organogenesis and Trauma, Department of Surgery, University of Texas Southwestern, Dallas, TX 75390, USA. [3]Department of Orthopaedics and Traumatology, University of Verona, Verona 37129, Italy. [4]Department of Neuroscience, Center for Advanced Pain Studies, University of Texas at Dallas, Dallas, TX 75080, USA. [5]Nuffield Department of Orthopaedics, Rheumatology and Musculoskeletal Sciences, Botnar Research Centre, Windmill Road, Oxford OX3 7LD, UK. [6]Department of Embryology, Carnegie Institution for Science, Baltimore, MD 21208, USA. [7]Department of Orthopaedics, University of Maryland, Baltimore, MD 21205, USA. [8]Baltimore Veterans Administration Medical Center, Baltimore, MD 21201, USA.
*Corresponding author. Email: awjames@jhmi.edu
†These authors contributed equally to this work.

immunostaining for β III-tubulin (TUBB3), combined with collagen imaging by second harmonic generation (SHG), showed TUBB3$^+$ peripheral nerve fibers coursing parallel to the tendon body and predominantly lying within the tendon sheath in the uninjured tendon (Fig. 1A and movie S1). After injury, sprouting and disorganization of nerve fibers were identified surrounding the injury site (Fig. 1B and movie S2). The temporal kinetics of peripheral nerve growth were further defined using sagittal sections of the Achilles tendon across a 42-day period after injury (Fig. 1C and fig. S1). Relative staining for TUBB3$^+$ nerves increased significantly over uninjured control as early as 7 days after injury, peaked after 14 days, and returned to baseline at day 42 ($P < 0.05$; Fig. 1D and fig. S1A). In our previous reports in bone regeneration, peripheral nerves and blood vessels showed close temporospatial interactions (*12*, *13*, *23*). To investigate this phenomenon in the context of tendon repair, immunostaining for cluster of differentiation 31 (CD31), a marker for blood vessels, was evaluated in adjacent sections of those for TUBB3 (Fig. 1, E and F, and fig. S1B). Similar to TUBB3, CD31 was observed within the tendon sheath at baseline, followed by a rapid increase in injury site over the first 14 days and returned to baseline after 42 days ($P < 0.05$; Fig. 1F). In agreement with our previous findings in bone regeneration, TUBB3 and CD31 staining was found near one another in the uninjured and injured tendon (fig. S2, A and B). Cell proliferation was next assessed by marker of proliferation Ki67 immunostaining on serial sections of the tendon injury site (Fig. 1, G and H, and fig. S1C). Temporal changes in the frequency of Ki67$^+$ cells mirrored those of neurovascularity of the injury site ($P < 0.05$; Fig. 1H). Most of peripheral nerves are NGF-responsive, TrkA-expressing neurons (*12*, *24*, *25*); therefore, changes in NGF expression were evaluated in a validated transgenic mouse model in which the NGF promoter controls the synthesis of enhanced green fluorescent protein (eGFP) (Fig. 1, I and J) (*13*, *26*). The uninjured Achilles tendon had little eGFP reporter activity; however, eGFP was increased by 7 days after injury, indicating increased expression of NGF ($P < 0.01$; Fig. 1, I and K). Immunofluorescent staining for TUBB3 showed peripheral nerves in the injury site within domains of NGF-eGFP reporter activity (Fig. 1J). Quantification of NGF reporter immunostaining indicated that the peak in NGF-eGFP expression was 7 days after injury ($P < 0.01$; Fig. 1K). Last, we assessed the cell types expressing the NGF reporter 7 days after tendon injury (Fig. 1, L and M, and fig. S3). As in other tissues (*13*), both eGFP$^+$ inflammatory and mesenchymal cells appeared to populate the tendon injury site, including broadly identified immune cells (CD45$^+$) and F4/80$^+$ macrophages (Fig. 1L and fig. S3), as well as mesenchymal cells expressing platelet-derived growth factor receptor α (PDGFRα), α–smooth muscle actin, and, to a lesser extent, tenomodulin (TNMD) (Fig. 1M and fig. S3), whereas CD31$^+$ endothelial cells (ECs) were not observed to express eGFP (fig. S3). In summary, NGF expression in macrophage and mesenchymal cells of the tendon injury site is followed by transient tendon-associated nerve sprouting and vascular and proliferative changes in the cascade of tendon repair.

Cell-specific *Ngf* knockout blunts Achilles tendon repair

Next, we queried the role of NGF on tendon repair, using previously generated transgenic animals with conditional *Ngf* deletion in most of mesenchymal cells ($Ngf^{Pdgfr\alpha}$) or in lysin motif$^+$ (LysM) myeloid cells (Ngf^{LysM}), in comparison with $Ngf^{fl/fl}$ (flox/flox) control mice (Fig. 2) (*13*). NGF immunohistochemistry on tissue sections of $Ngf^{Pdgfr\alpha}$ or Ngf^{LysM} injury sites confirmed absence of NGF in cells expressing the reporter (Fig. 2A). Hematoxylin and eosin (H&E)–stained sagittal sections of the injury site (Fig. 2B) and tendon histologic scoring (*27*) showed a significant healing impairment in both $Ngf^{Pdgfr\alpha}$ ($P < 0.05$) and Ngf^{LysM} ($P < 0.01$) animals (Fig. 2C and fig. S4; results stratified by sex in fig. S5). In agreement with histological findings, enhanced micro–computed tomography (μCT) images and quantification of healed tendon volume (dark signal) confirmed a tendon deficit in both $Ngf^{Pdgfr\alpha}$ and Ngf^{LysM} animals (Fig. 2, D and E). Immunofluorescent staining of the injury sites by axial sections 14 days after injury showed that conditional deletion of the primary neurotrophin *Ngf* caused a significant reduction in TUBB3$^+$ at the injury site in both $Ngf^{Pdgfr\alpha}$ and Ngf^{LysM} animals ($P < 0.001$; Fig. 2, F and G). Changes in innervation were accompanied by reductions in CD31$^+$ blood vessels in the injured areas in $Ngf^{Pdgfr\alpha}$ and Ngf^{LysM} tendons in comparison with the $Ngf^{fl/fl}$ controls ($P < 0.05$; Fig. 2, H to I). Alterations in cell proliferation and TNMD$^+$ tenocyte differentiation were next assessed (Fig. 2, J to M). A reduction in Ki67$^+$ cell number was found in $Ngf^{Pdgfr\alpha}$ and Ngf^{LysM} injured tendons in comparison with $Ngf^{fl/fl}$ control ($P < 0.01$; Fig. 2, J and K). TNMD immunostaining likewise was significantly reduced in $Ngf^{Pdgfr\alpha}$ and Ngf^{LysM} animals in the injured areas around the tendon body in comparison with $Ngf^{fl/fl}$ control ($P < 0.001$; Fig. 2, L and M). Thus, mice with *Ngf* conditional knockout in either mesenchymal or myeloid cell populations show impaired neurovascular response to tendon injury, accompanied by deficits in cell proliferation and tenocyte differentiation.

Inhibition of TrkA activity reduces tendon repair

Most of sensory neurons that innervate skeletal structures express the high-affinity receptor for NGF, TrkA (*28*). In prior studies, we leveraged the availability of a previously characterized chemical genetic approach to temporally inhibiting TrkA catalytic activity by administration of a small-molecule inhibitor in mice (*12*). $TrkA^{F592A}$ mice have a point mutation in exon 12 of the neurotrophic receptor tyrosine kinase 1 (*Ntrk1*) gene, allowing for TrkA kinase inhibition by the small molecule 1-tertbutyl-3-naphthalen-1-ylmethyl-1H-pyrazolo[3,4-d]pyrimidin-4-ylemine (1NMPP1), whereas $TrkA^{WT}$ mice are insensitive to 1NMPP1 (*29*) and have no phenotypic changes in their Achilles tendon at baseline (*25*). Similar to *Ngf* conditional knockout animals, tendon healing, as determined by H&E staining, histologic scoring (Fig. 3, A and B, and fig. S6), and enhanced μCT imaging (Fig. 3, C and D), was significantly reduced in 1NMPP1-treated $TrkA^{F592A}$ animals in comparison with age-matched, 1NMPP1-treated $TrkA^{WT}$ 14 days after injury ($P < 0.05$; Fig. 3, A to D; results stratified by sex in fig. S5). Immunofluorescent staining for neurovascularity of the injury site using axial sections of injured $TrkA^{WT}$ and $TrkA^{F592A}$ mice showed that TrkA inhibition led to a significant reduction of TUBB3$^+$ nerves ($P < 0.05$; Fig. 3, E and F) and a reduction in CD31$^+$ ECs in the injured area ($P < 0.05$; Fig. 3, G and H). Cell proliferation and tenocyte differentiation were assessed within the injured area of TrkA-inhibited animals by Ki67 and TNMD immunostaining, respectively (Fig. 3, I to L). Ki67$^+$ ($P < 0.05$; Fig. 3, I and J) and TNMD$^+$ cells were significantly reduced in $TrkA^{F592A}$ tendon injuries relative to those in $TrkA^{WT}$ ($P < 0.05$; Fig. 3, K and L). Thus, inhibition of TrkA kinase activity during tendon repair led to deficits in neoinnervation and regeneration that largely phenocopied *Ngf* conditional gene deletions.

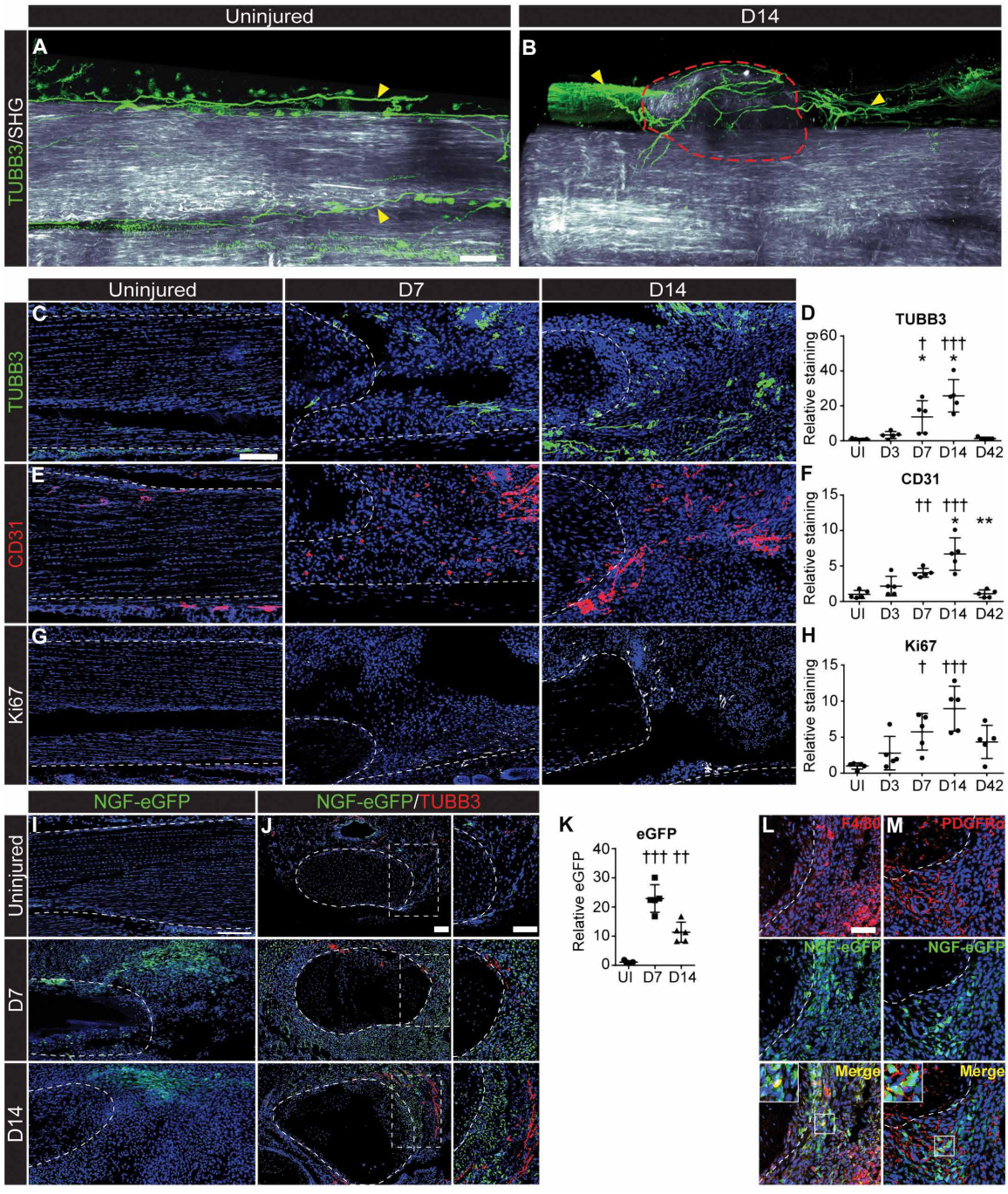

Fig. 1. Neurovascular ingrowth is an early response to murine Achilles tendon injury. (**A** and **B**) Whole-mount imaging of the murine Achilles tendon with SHG (gray scale) for tendon extracellular matrix and TUBB3 immunostaining (green). Yellow arrowheads indicate nerve fibers, and red dashed line indicates injured area. (**C**) Representative TUBB3 immunofluorescent staining (green) in sagittal sections of the Achilles tendon before and after injury; additional images are in fig. S1. (**D**) Quantification of relative staining of TUBB3 in uninjured (UI) and 3 to 42 days after injury. (**E**) Endothelial marker CD31 immunofluorescent staining (red) and (**F**) quantification of CD31 staining. (**G**) Proliferation marker Ki67 immunofluorescent staining (white) and (**H**) quantification of Ki67 staining. (**I**) NGF-eGFP reporter (green) in sagittal sections of the tendon before and after injury. (**J**) NGF-eGFP reporter (green) and TUBB3 immunofluorescent staining (red) on axial sections. (**K**) Quantification of NGF-eGFP reporter staining. (**L** to **Q**) Immunofluorescent staining for cell-specific markers on NGF-eGFP reporter sections 7 days after injury, including (L) F4/80 and (M) platelet-derived growth factor receptor α (PDGFRα). Green (NGF-eGFP), red (F4/80 or PDGFRα), and merged channels are shown separately. Nuclei are visualized with 4′,6-diamidino-2-phenylindole (DAPI) staining (blue). Graphs show means ± 1 SD, and data points represent individual animal measurements. $n = 5$ mice per time point. †$P < 0.05$; ††$P < 0.01$; †††$P < 0.001$ compared with UI; *$P < 0.05$; **$P < 0.01$ compared with day 7. One-way ANOVA with Tukey's post hoc test. Scale bars, 100 μm. White dashed rectangles indicate areas of higher magnification; curved dashed white lines indicate the margins of the Achilles tendon.

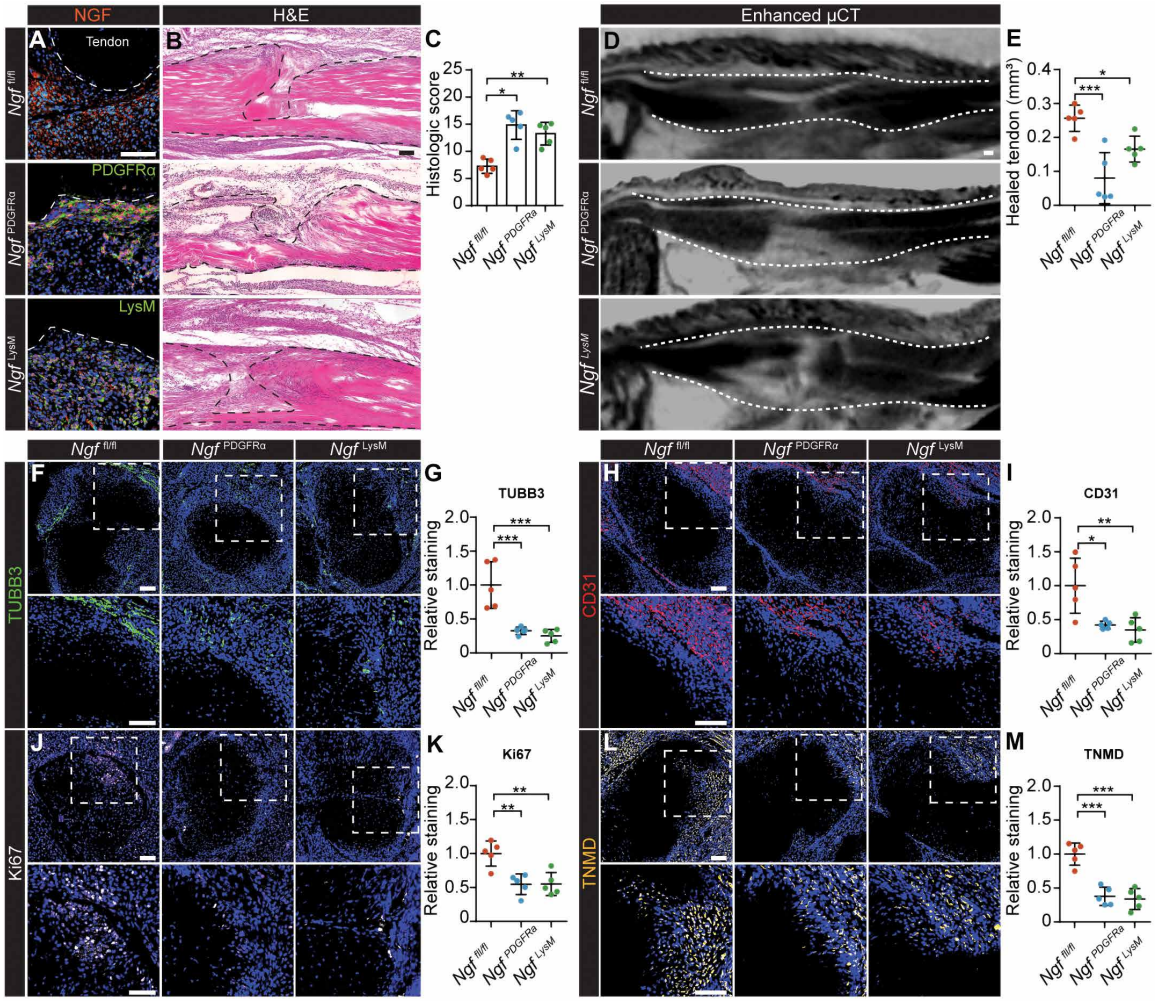

Fig. 2. *Ngf* deletion in myeloid or mesenchymal cells inhibits tendon neurovascularization and repair. (**A**) Immunohistochemical evaluation of efficiency of conditional *Ngf* deletion in axial sections 14 days after injury (NGF, red). Cells expressing PDGFRα or LysM reporters appear green. Nuclei are visualized with DAPI staining (blue). (**B**) H&E staining performed on sagittal sections of the injury site in $Ngf^{fl/fl}$, $Ngf^{PDGFR\alpha}$, and Ngf^{LysM} animals, 14 days after injury. (**C**) Histological score of healing in sagittal sections. Scoring parameters detailed in fig. S4. (**D**) Enhanced μCT shown in sagittal cross section. Dashed white lines indicate margins of tendon. (**E**) μCT quantification of Achilles tendon volume within the injured area 14 days after injury. (**F**) TUBB3 immunofluorescent staining (green) for injury site innervation in axial sections and (**G**) quantification. **H**) CD31 immunofluorescent staining (red) for injury site vascularization in axial sections and (**I**) quantification. (**J**) Ki67 immunofluorescent staining for injury site proliferation in axial sections and (**K**) quantification. (**L**) TNMD immunofluorescent staining within axial sections of tendon injury site and (**M**) quantification. Graphs show means ± 1 SD, and data points represent individual animal measurements. $n = 5$ mice per genotype. $^*P < 0.05$; $^{**}P < 0.01$; $^{***}P < 0.001$ relative to $Ngf^{fl/fl}$ control. One-way ANOVA with Tukey's post hoc test. Scale bars, 100 μm. White dashed rectangles indicate areas of higher magnification.

Single-cell and spatial RNA sequencing describe the transcriptional landscape of the injured tendon

To determine the cellular and molecular landscape that leads to tendon repair deficits with inhibition of TrkA in peripheral nerves, we performed a combination of single-cell RNA sequencing (scRNA-seq) and spatial transcriptomic analysis (spatial-seq) on the Achilles injury site of $TrkA^{WT}$ and $TrkA^{F592A}$ animals. We profiled the transcriptome of 22,075 single cells from $TrkA^{WT}$ and $TrkA^{F592A}$ injured Achilles tendons. Using unbiased clustering, we distinguished seven clusters with differing cell population markers (fig. S7, A and B) and relatively equal cell distribution between wild-type (WT) and F592A mouse genotypes (fig. S7, C and D). Mesenchymal cells represented 10,663 of the total analyzed cells and were distributed across four subclusters (Fig. 4A) defined by characteristic gene markers: subcluster 1, tendon progenitor cell [tenascin XB (*Tnxb*), *Cd34*, *Cd248*, and *Tppp3*]; subcluster 2, peripheral tendon cell [*Tppp3*, lipoprotein lipase (*Lpl*), and insulin-like growth factor 2 (*Igf2*)]; subcluster 3, pretenocyte [tenascin N (*Tnn*), retinol binding protein 4 (*Rbp4*), and collagen type XVIII α1 chain (*Col18a1*)]; and subcluster 4, tenocyte [*Tnmd*, scleraxis (*Scx*), and cartilage intermediate layer protein 2 (*Cilp2*)] (Fig. 4, A and B, and fig. S7, E and F). For spatial-seq, 2027 spatial spots in the tendon and injury site were evaluated for the number of features (nFeatures) and the number of unique molecular identifiers (nCount) (fig. S8). Tendon expressed 2930, whereas the injury site expressed 7047 unique transcripts per spot (fig. S8). The spatial spots were manually segmented into four regions of interest based on H&E staining including (1) the tendon proper, (2) the mid-injury (M), (3) the peripheral injury (P), and (4)

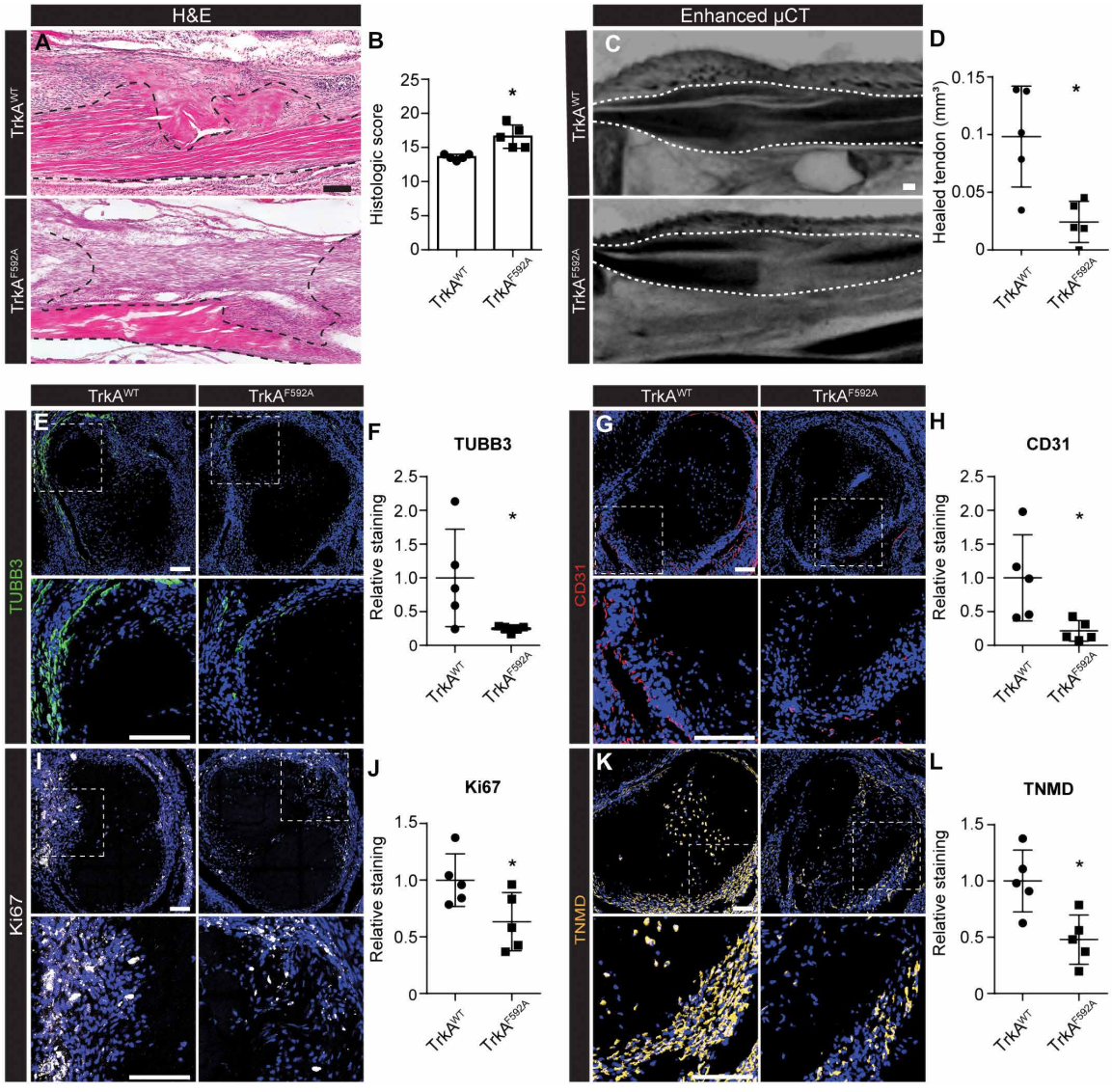

Fig. 3. Temporally controlled TrkA inhibition reduces tendon neurovascularization and repair. (**A**) H&E staining on sagittal sections of the injury site; black dashed lines indicate margins of tendon. (**B**) Histological score of healing in sagittal sections. (**C**) Enhanced μCT shown in sagittal cross section; white dashed lines indicate margins of tendon. (**D**) μCT quantification of Achilles tendon volume within the injured area. (**E**) Innervation of the injury site in axial sections (TUBB3, green) and (**F**) relative staining quantification. (**G**) Vascularization of the injury site (CD31, red) and (**H**) relative staining quantification. (**I**) Cell proliferation of the injury site (Ki67, white) and (**J**) quantification. (**K**) TNMD staining (yellow) within axial sections of the tendon injury site and (**L**) relative staining quantification. Nuclei are visualized with DAPI staining (blue). Graphs show means ± 1 SD, and data points represent individual animal measurements. *$P < 0.05$ in relation to TrkA^{WT} control using a two-tailed Student's *t* test. Scale bars, 100 μm. White dashed rectangles indicate areas of higher magnification. $n = 5$ mice per genotype.

the deep injury (D) (Fig. 4C). To rationally assess scRNA-seq and spatial-seq datasets jointly, it was necessary to validate that the four mesenchymal subclusters defined by scRNA-seq were present and adequately populated the four manually segmented spatial regions of interest. The predicted mesenchymal cellular identities as defined by scRNA-seq subclustering were compared with the cellular identities from the four manually splined spatial-seq regions. A high degree of correlation was observed between the cell identities defined by scRNA-seq and spatial-seq as observed by the prediction score (Fig. 4D). The tendon proper and mid-injury area were predicted to be populated by tenocytes and pretenocytes, respectively. The peripheral and deep injury areas were predicted to be most populated by peripheral and progenitor cells, respectively (Fig. 4E and fig. S9). As further validation, gene ontology (GO) term analysis was performed separately across scRNA-seq and spatial-seq datasets. GO analysis was evaluated in regions associated with the intact tendon or tenocytes (spatial-seq, region 1; scRNA-seq, subcluster 4) (Fig. 4F) or regions associated with the injury site transcriptional data (spatial-seq, regions 2 to 4; scRNA-seq, subclusters 1 to 3) (Fig. 4G). Overall, patterns in GO term enrichment were evident across scRNA-seq and spatial-seq datasets, where, for example, tendon areas were enriched for GO terms such as cell adhesion and response to hypoxia, whereas the injured areas showed terms related to cell migration, angiogenesis, neural projection development, and transforming

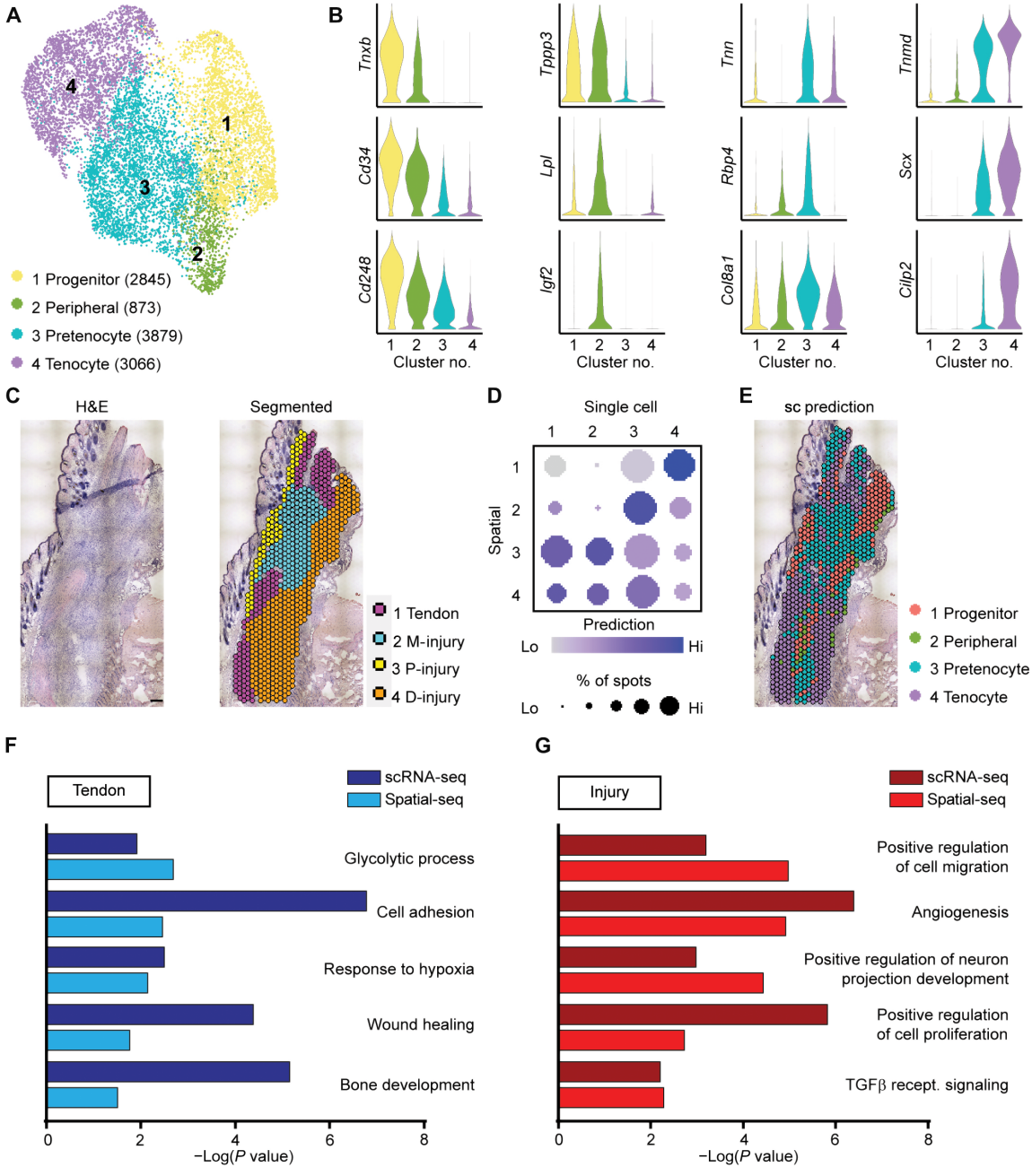

Fig. 4. A combination of single-cell sequencing and spatial sequencing revealed a hierarchical and topographical distribution of mesenchymal cells within the tendon injury site. (**A**) Uniform Manifold Approximation and Projection (UMAP) projection of mesenchymal cell subclusters by scRNA-seq, including (1) progenitor cells, (2) peripheral cells, (3) pretenocytes, and (4) tenocytes. (**B**) Violin plots for characteristic markers of mesenchymal subclusters by scRNA-seq, including progenitor cell markers *Tnxb*, *Cd34*, *Cd248*, and *Tppp3*; peripheral cell markers *Lpl* and *Igf2*; pretenocyte markers *Tnn*, *Rbp4*, and *Col18a1*; and tenocyte markers *Tnmd*, *Scx*, and*Cilp2*. (**C**) H&E-stained section overlayed with spatial-seq spots manually segmented by location, including (1) tendon, (2) mid-injury (M), (3) peripheral injury (P), and (4) deep injury (D). (**D**) Correlation of mesenchymal subclusters as defined by scRNA-seq to spatial segmentation data, shown by dot plot. (**E**) Predicted localization of scRNA-seq mesenchymal cell subclusters onto spatial sequencing data. (**F**) GO term enrichment correlating scRNA-seq to spatial sequencing in tendon (spatial-seq) or tenocytes (subcluster 4, scRNA-seq). (**G**) GO term enrichment correlating scRNA-seq to spatial sequencing in the injury site (spatial-seq) or progenitor cells (subcluster 1, scRNA-seq). Scale bar, 200 μm. $n = 3$ mice per genotype for single-cell RNA sequencing; $n = 4$ per genotype for spatial sequencing.

growth factor–β (TGFβ) receptor signaling (Fig. 4, F and G). Thus, a combination of scRNA-seq and spatial-seq after murine tendon injury yielded a conserved integrated spatial landscape defining the transcriptomic profile across mesenchymal cell populations.

Inhibition of TrkA activity causes alterations in inflammatory and TGFβ signaling at the tendon repair site

To more precisely describe the molecular alterations caused by TrkA inhibition during tendon healing, further stratification of scRNA-seq

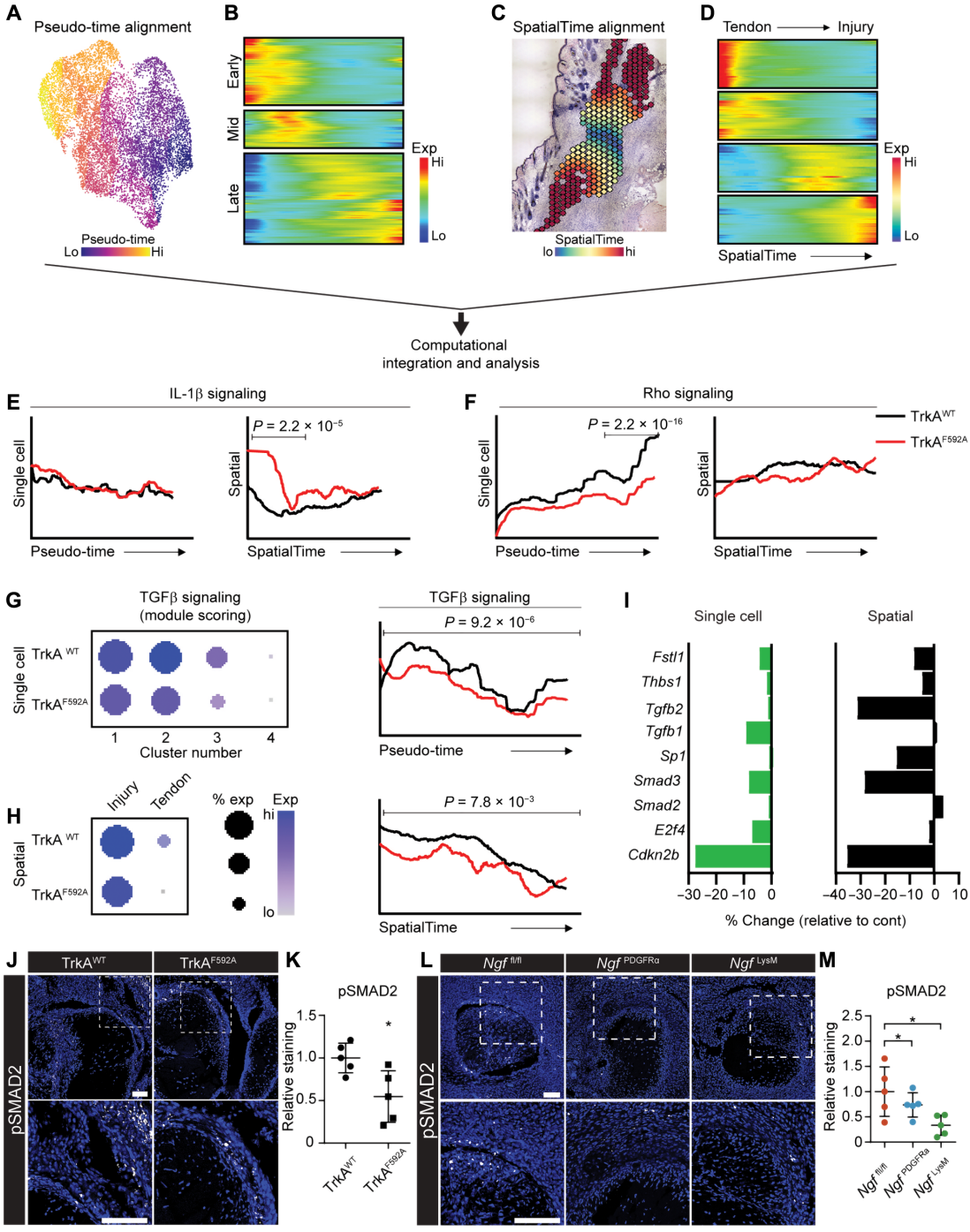

Fig. 5. Dysregulation of inflammatory and TGFβ signaling with deficient neural ingrowth into the tendon repair site. (**A**) UMAP projection of mesenchymal cell subclusters across pseudo-time by scRNA-seq. (**B**) Heatmap displaying differential gene expression across pseudo-time in the mesenchymal subcluster. (**C**) SpatialTime alignment of tendon- and injury-associated spatial spots. (**D**) Heatmap displaying differential gene expression across SpatialTime in the mesenchymal subcluster, followed by computational integration and analyses. (**E**) IL-1β signaling module across pseudo-time (left) and SpatialTime (right), among either TrkA^{WT} (black) or TrkA^{F592A} (red) animals. (**F**) Rho signaling across pseudo-time (left) and SpatialTime (right) among either TrkA^{WT} or TrkA^{F592A} animals. (**G**) Dysregulation of TGFβ signaling with TrkA inhibition, as determined by gene module scores among mesenchymal cells. TGFβ signaling is shown by mesenchymal subcluster (left) or across pseudo-time (right). (**H**) Dysregulation of TGFβ signaling by spatial-seq with TrkA inhibition, as determined by gene module scores across spatial spots within the injury site and tendon (left) and across SpatialTime (right). %Exp represents the percentage of cells or spots that express the genes related to the pathway indicated. The Exp color indicates the extent of expression. (**I**) Relative change among TGFβ-associated genes among TrkA^{F592A} animals in comparison with TrkA^{WT} in the progenitor cell subcluster and tendon/injury area as determined by either in the Mes subcluster by scRNA-seq (left) or at the tendon/injury area by spatial sequencing (right). (**J**) pSMAD2 immunofluorescent staining among TrkA^{WT} and TrkA^{F592A} animals, 14 days after injury, and (**K**) quantification. (**L**) pSMAD2 immunofluorescent staining among *Ngf*$^{fl/fl}$, *Ngf*^{PDGFRα}, and *Ngf*^{LysM} animals 14 days after injury and (**M**) quantification. Graphs show means ± 1 SD, and data points represent individual animal measurements. *$P < 0.05$ in comparison to TrkA^{WT} in (H) with a two-tailed Student's *t* test and *Ngf*$^{fl/fl}$ in (J) with a one-way ANOVA with Tukey's post hoc test. Scale bars, 100 μm. White dashed rectangles indicate areas of higher magnification. $n = 5$ mice per genotype.

and Spatial-seq analysis was performed (Fig. 5). For scRNA-seq, the four mesenchymal subclusters were identified and aligned along pseudo-time from progenitor cell to tenocyte (Fig. 5, A and B) (*30*). In an analogous method, spatial spots were categorized by distance from the midpoint of the tendon injury site. The location relative to the injury was then aligned across tendon "SpatialTime," adapted from our prior work in bone tissue such that early SpatialTime represents injured regions and late SpatialTime represents normal tendon (Fig. 5, C and D) (*30*). These tools allow the comparison of the genotypes across cell clusters and location relative to the injury. Comparison of discrete signaling pathways using modules of genes (table S1) demonstrated unique trends across pseudo-time and

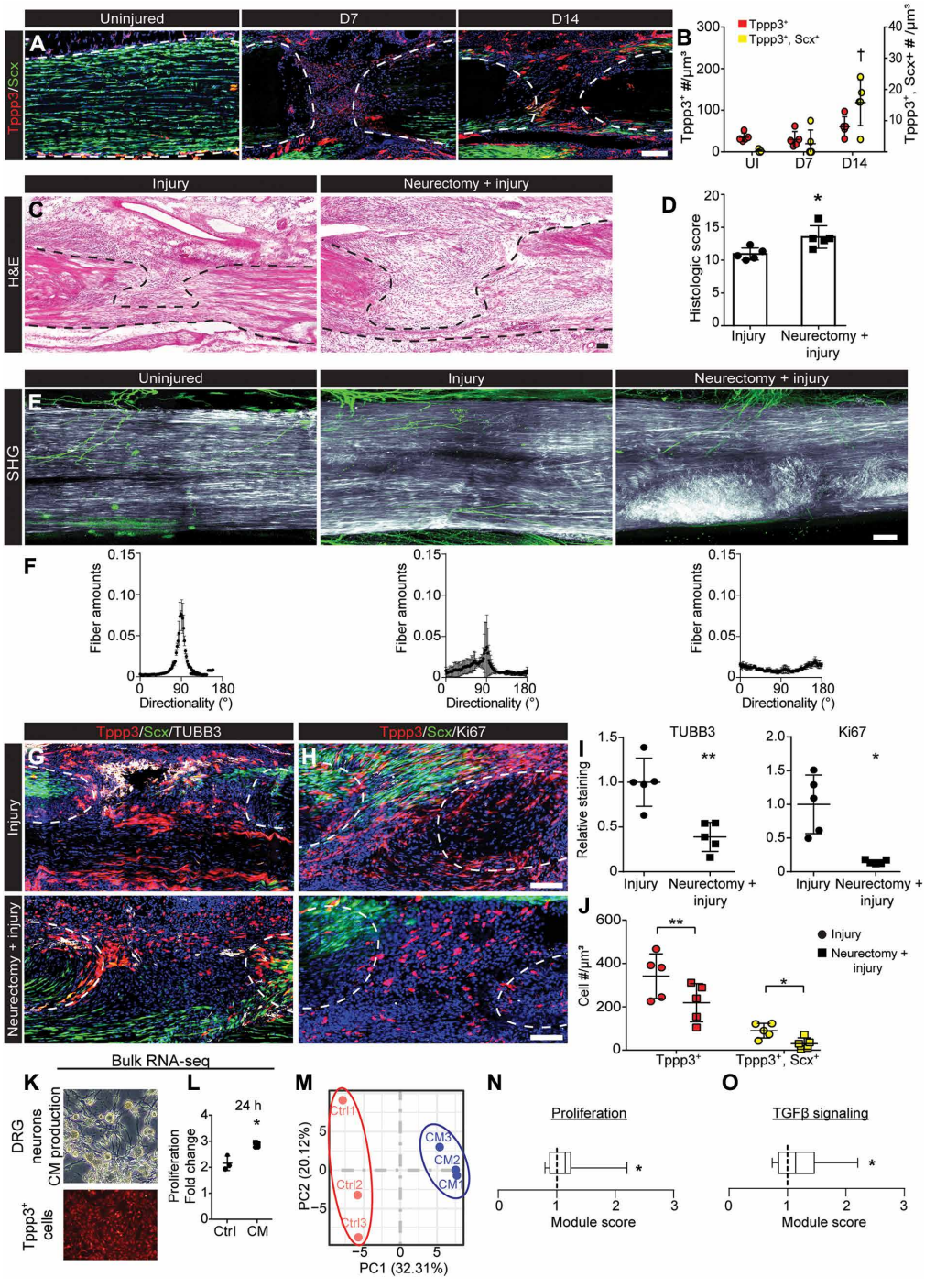

Fig. 6. Sural neurectomy inhibits *Tppp3*$^+$ TSPC expansion and tendon repair. (**A**) Sagittal sections of the tendon, up to 14 days after injury. (**B**) Quantification of *Tppp3*$^+$ and dual *Tppp3*$^+$/*Scx*$^+$ cell number before (UI) and after injury. (**C**) H&E staining performed on sagittal sections of the tendon injury site in injured or neurectomized injured animals. (**D**) Histological healing score within injured or neurectomized injured animals. (**E**) SHG whole-mount imaging of the Achilles tendon with TUBB3 immunostaining. (**F**) Quantification of collagen fiber directionality shown in (E). (**G** to **J**) *Tppp3*-tdT-CreER^{T2};*Scx*-GFP animals underwent sham or sural neurectomy surgery, followed by tendon injury after 7 days. Animals were analyzed 14 days after tendon injury. (G) Neural ingrowth assessed by TUBB3 immunostaining. (H) Cell proliferation assessed by Ki67 immunostaining and (I) quantification of (G) and (H). (J) Quantification of *Tppp3*$^+$ (red) and *Tppp3*$^+$*Scx*$^+$ cells (yellow) in tissue sections corresponding to (G) and (H) among injured or neurectomized injured animals. (**K**) Lumber DRG neuron culture for CM production (top) and *Tppp3*$^+$ sorted cells exposed to control medium or neural CM. (**L**) Quantification of proliferation by 3-(4,5-dimethylthiazol-2-yl)-5-(3-carboxymethoxyphenyl)-2-(4-sulfophenyl)-2H-tetrazolium) (MTS) assay 24 hours after incubation with neural CM or control unconditioned medium. (**M** to **O**) Transcriptomic analysis of *Tppp3*$^+$ cells treated with or without neural CM for 24 hours. (M) PCA of total RNA sequencing of *Tppp3*$^+$ cells treated with neural CM (blue) or control unconditioned medium (red) for 24 hours. (N and O) Analysis of module scores related to (N) cell proliferation and (O) TGFβ signaling. Graphs show means ± 1 SD, and data points represent individual animal measurements. $n = 5$ mice per group. †$P < 0.05$ in comparison with UI with a one-way ANOVA and Tukey's post hoc test. *$P < 0.05$; **$P < 0.01$ in comparison with injured with a two-tailed Student's *t* test. Scale bars, 100 µm. White dashed lines indicate Achilles tendon margins.

SpatialTime between TrkA^{WT} and TrkA^{F592A} (Fig. 5, E to I). For example, interleukin-1β (IL-1β) signaling module was up-regulated among TrkA^{F592A} animals in spatial-seq, and its activation was spatially dependent and enriched in early SpatialTime corresponding to the injury site, suggesting that TrkA signaling is important for the regulation of IL-1β in the injury site (Fig. 5E). In contrast, Rho signaling pathway, which is important for neurite axon pathfinding, outgrowth, and differentiation (*31*), was down-regulated among TrkA^{F592A} animals in scRNA-seq analysis, with a significant reduction in late pseudo-time ($P < 0.05$), but no difference in SpatialTime, reflecting a molecular change dependent on cell phenotype rather than spatial localization (Fig. 5F). Of the examined signaling pathways (fig. S10 and table S1), Wnt and bone morphogenetic protein (BMP) modules were similar in pseudo-time (fig. S10A, left) and different in SpatialTime (fig. S10A, right), whereas hypoxia-inducible factor 1 (HIF-1) and fibroblast growth factor (FGF) modules were different between genotypes in pseudo-time (fig. S10B, left) and similar in SpatialTime (fig. S10B, right). The TGFβ pathway was dysregulated in TrkA^{F952A} animals in both pseudo-time and SpatialTime (Fig. 5, G and H). In TrkA^{WT} animals, scRNA-seq demonstrated

higher TGFβ signaling activation in mesenchymal subclusters 1 and 2, corresponding to higher expression in early pseudo-time (progenitor and peripheral tendon cells) compared with TrkA^{F952A} animals (Fig. 5G). Consistent with this finding, regulatory network analysis identified transcription factors regulated by TGFβ signaling to be most active among early pseudo-time (fig. S11A), including *Myc*, *Cebpb*, and *Junb* (fig. S11B). In TrkA^{WT} animals, TGFβ signaling activation was highest in the injury site (early SpatialTime) compared with the tendon (late SpatialTime). Loss of TrkA activity in TrkA^{F952A} animals caused a reduction in TGFβ signaling across SpatialTime, suggesting that TrkA signaling is important for TGFβ activation in the injury (Fig. 5H). Differentially expressed genes (DEGs) related to TGFβ signaling pathway were further analyzed in TrkA^{WT} versus TrkA^{F952A} animals (Fig. 5I). Genes including *Cdkn2b*,

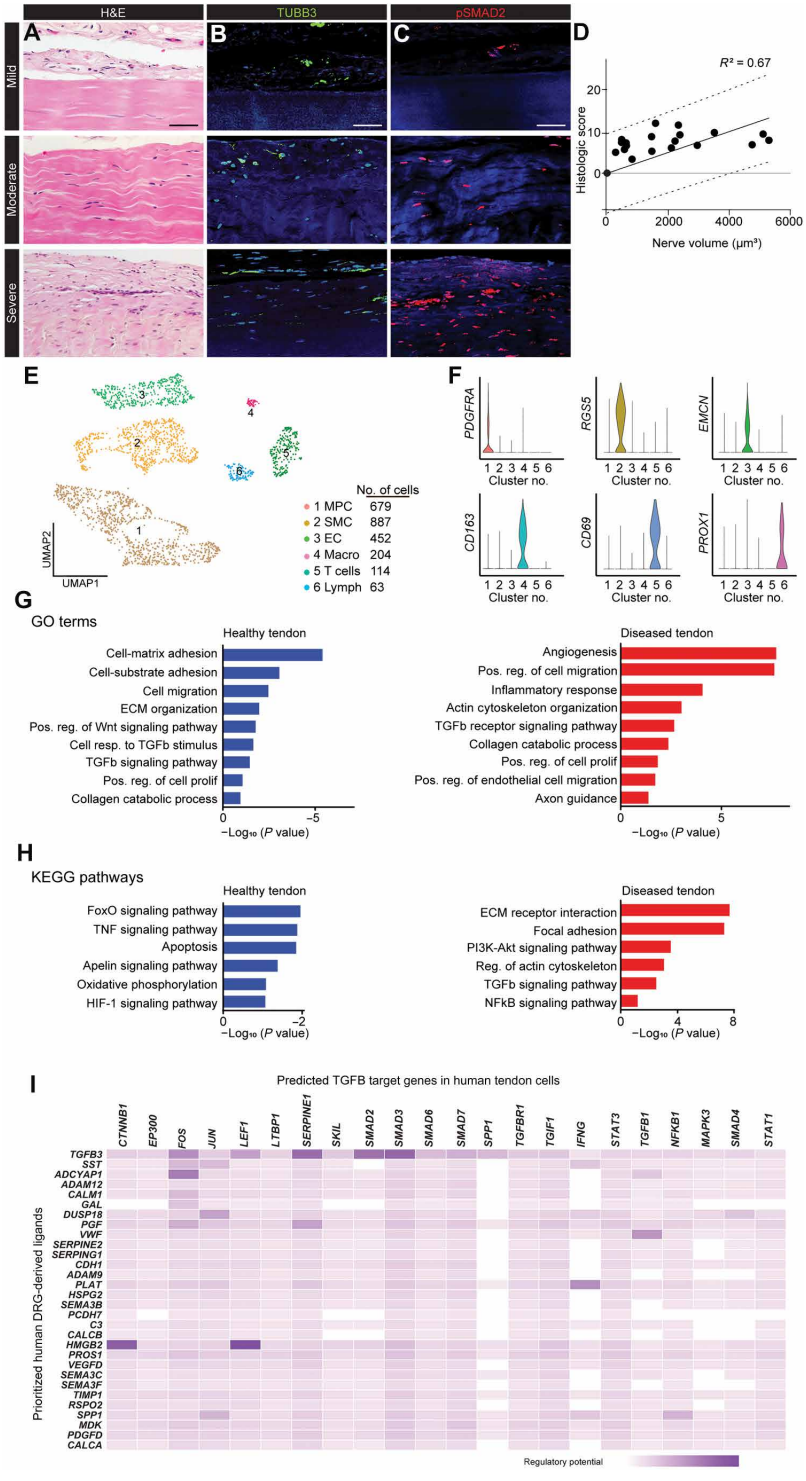

Fig. 7. Human tendinopathy is associated with innervation and TGFβ signaling dysregulation. (**A** to **D**) Histologic assessments of peripheral nerves and TGFβ signaling among human biceps tendon samples. (A) Representative H&E staining performed on sagittal sections of a human tendon, demonstrating mild, moderate, and severe tendinopathy. (B) Human tendon innervation, assessed by TUBB3 immunofluorescent staining. (C) TGFβ signaling, assessed by pSMAD2 immunofluorescent staining. (D) Linear correlation and 95% prediction band between histologic score and nerve volume quantified in human tendon samples. Each dot represents a single tendon image analyzed. A higher histologic score indicates more severe tendinopathy. (**E** to **I**) scRNA-seq of healthy and diseased human tendon tissue. (E) UMAP projection of total cells isolated from human tendons by scRNA-seq, including mesenchymal progenitor cells (MPCs), smooth muscle cells (SMCs), ECs, macrophages (Macro), T cells, and lymphatic cells (lymph). (F) Violin plot of characteristic markers for each cluster. (G) Representative GO term enrichment for healthy and diseased tendons. (H) Representative KEGG pathway enrichment among human tendon cells. (I) Interaction plot depicting the predicted human DRG-derived ligands with predicted downstream targets present in tendon MPCs. Graphs show data points for $n = 20$ individual patients biceps tendon samples used for histology. $n = 2399$ human tendon cells obtained from (*40*). $n = 1757$ human DRG neurons analyzed, obtained from (*41*). PI3K, phosphatidylinositol 3-kinase.

Smad2, *Smad3*, *Tgfb1*, *Tgfb2*, *Thbs1*, and *Fslt1* were down-regulated in both scRNA-seq and spatial-seq transcriptomic datasets (additional DEGs shown in tables S2 to S5).

To computationally reconstruct the potential cellular communication that exists between TrkA^{+} neurons and mesenchymal cells of the tendon injury site and further investigate TGFβ signaling, we computationally integrated a second scRNA-seq dataset of mouse lumbar dorsal root ganglia (DRG) cells (*32*) with those of our identified tendon-associated mesenchymal cell subclusters (fig. S12, A and B). The R package NicheNet (*33*) was used to reconstruct potential neural-to-mesenchymal cell signaling by ligand-receptor matching (fig. S12C). TGFβ ligands (*Tgfb1* and *Tgfb3*), *Gdf11*, BMPs (*Bmp3* and *Bmp8a*), and neuropeptides such as *Tac1* were expressed in *Ntrk1* (TrkA) expressing DRG neurons, and their corresponding receptors were expressed in tendon injury site mesenchymal cells (fig. S12D). Of these, *Tgfb1* and *Tgfb3* were highly predicted to play a role in neural-to-mesenchymal paracrine interaction based on regulatory potential (fig. S12E).

Last, these alterations in TGFβ signaling across transcriptomic datasets were validated by staining for phospho-SMAD2 (pSMAD2), a downstream transcription factor of TGFβ signaling pathway, in tissue sections of tendon injury sites with TrkA inhibition or *Ngf* conditional deletion (Fig. 5, J to M). Injured tendon tissue exhibited high pSMAD2 immunostaining in TrkA^{WT} mice and a significant reduction of immunoreactivity in TrkA^{F592A} animals ($P < 0.05$; Fig. 5, J and K). Similarly, pSMAD2 immunofluorescent staining showed a significant reduction in *Ngf*$^{Pdgfr\alpha}$ and *Ngf*^{LysM} conditional knockout mice when compared with *Ngf*$^{fl/fl}$ controls ($P < 0.05$; Fig. 5, I and J). Thus, defective innervation in the context of the loss of NGF-TrkA signaling was associated with downstream reductions in TGFβ signaling, with our results implicating TGFβ ligands themselves as neural-derived secreted factors.

Alterations in inflammatory and EC phenotypes with inhibition of TrkA activity

Tendon repair outcomes are not only associated with progenitor cell proliferation and differentiation but also influenced by other niche factors, such as tendon associated vascularity (*34*) and immune cell infiltration (*35*, *36*). Therefore, we compared EC transcriptomic profiles in TrkA^{WT} versus TrkA^{F592A} injury sites (fig. S13A). Gene markers associated with endothelial tip cell phenotype, which are distinct ECs present in the nascent sprout of blood vessels (*37*, *38*), were assessed, including delta-like canonical Notch ligand 4 (*DLL4*), angiopoietin 2 (*ANGPT2*), and nidogen-2 (*NID2*). Tip cell markers were greatly reduced in TrkA^{F592A} ECs; however, genes associated with vessel maturation and hypoxia were highly enriched (fig. S13B and table S6). In addition, loss of TrkA activity caused a decrease in individual gene markers of proliferation and cell cycle in TrkA^{F592A} ECs (fig. S13C). Computational modeling was used to map the predicted location of ECs from scRNA-seq within the spatial-seq data (fig. S13D). The analysis revealed that in TrkA^{WT} mice, there was an enriched distribution of ECs at the anterior and posterior areas of the injured Achilles tendon; however, with inhibition of TrkA activity, there was a loss of vascularization in these areas (fig. S13, D and E). GO term enrichment analysis in TrkA^{F592A} versus TrkA^{WT} ECs was performed (fig. S13F). Consistent with prior findings in other models (*37*), TrkA^{WT} ECs showed enrichment in GO terms related to regulation of growth, extracellular matrix (ECM) organization, insulin-like growth factor receptor signaling, and cell proliferation. In contrast, TrkA^{F592A} ECs had GO term enrichment for glycolysis, cell response to hypoxia, positive regulation of apoptosis, and inflammation (fig. S13F). Last, module scores of curated gene sets confirmed a decrease in transcripts associated with TGFβ signaling activation in TrkA^{F592A} ECs (fig. S13G). A combination of scRNA-seq and spatial-seq identified defects in EC proliferation and vascular growth during tendon injury repair with inhibition of TrkA activity.

Macrophages in TrkA^{WT} and TrkA^{F592A} animals were analyzed by single cell and spatial transcriptomics (fig. S13H). GO term enrichment analysis among TrkA^{WT} macrophages showed terms related to tissue healing, including positive regulation of fibroblast proliferation, and collagen biosynthesis, connective tissue replacement, and angiogenesis (fig. S13I). In contrast, TrkA^{F592A} macrophages showed GO term enrichment related to inflammation and negative regulation of endothelial proliferation and growth (fig. S13I). Integration of scRNA-seq and spatial-seq datasets was performed to map the predicted spatial distribution of macrophages within the tendon injury site (fig. S13J). There was a predicted enrichment in macrophages within all manually splined compartments of the injured tendon in both TrkA^{WT} and TrkA^{F592A} mice compared with uninjured (fig. S13, J and K). In agreement with scRNA-seq analysis, spatial-seq showed that TrkA^{WT} tissue macrophage–enriched spots displayed GO terms associated with a prohealing phenotype, including cell migration and positive regulation of cell proliferation. In injured tissue expressing TrkA^{F592A}, a proinflammatory phenotype with GO terms including response to lipopolysaccharide and reactive oxygen species was observed in macrophage-enriched spots (fig. S13L). TGFβ activator and inhibitor module scores confirmed a decrease in transcripts associated with activation of TGFβ signaling in TrkA^{F592A} macrophages (fig. S13M). Together, these data suggest that inhibition of TrkA activity in the context of tendon injury resulted in consistent shifts in macrophage transcriptional phenotype, suggesting changes from a "regenerative" to an "inflammatory" phenotype by both scRNA-seq and spatial-seq.

Sural neurectomy impairs *Tppp3*$^{+}$ TSPC proliferation and tendon repair

Prior studies have implicated TSPCs expressing *Tppp3* as integral to mouse tendon repair (*39*). Next, TSPC reporter mice, which carry an inducible reporter under the *Tppp3* promoter (*Tppp3*$^{ECE/+}$;R26R^{tdT}-CreER^{T2}) (*39*) were crossed with mice expressing a constitutive GFP reporter under the *Scx* promoter to obtain double transgenic *Tppp3*$^{ECE/+}$;R26R^{tdT}-CreER^{T2};*Scx*-GFP reporter mouse. The double reporter mice, which have labeled Tppp3^{+} cells (red) and Scx^{+} cells (green), were evaluated at baseline and after Achilles tendon injury to visualize *Scx* expression and *Tppp3* lineage cell types (Fig. 6, A and B). Fluorescent detection and quantification of reporter activity demonstrated a gradual increase in dual *Tppp3*$^{+}$*Scx*$^{+}$ cells by day 14 after tendon injury (Fig. 6B). The effects of ipsilateral neurectomy of the sural nerve (which carries sensory fibers only) in *Tppp3*$^{ECE/+}$;R26R^{tdT}-CreER^{T2};*Scx*-GFP reporter mice was assessed (Fig. 6, C to J). To validate effective neurectomy, TUBB3^{+} nerves were evaluated in the tendon 7 days after sham denervation (fig. S14A) or surgical neurectomy (fig. S14B). Sural neurectomy resulted in a significant reduction of TUBB3^{+} staining ($P < 0.05$; fig. S14C). Ipsilateral tendon injury was performed 7 days after sural neurectomy, and analysis of injured or neurectomized injured animals was performed 14 days thereafter. H&E staining of longitudinal sections showed the neurectomized group had less organized collagen fibers, higher cellularity, and a

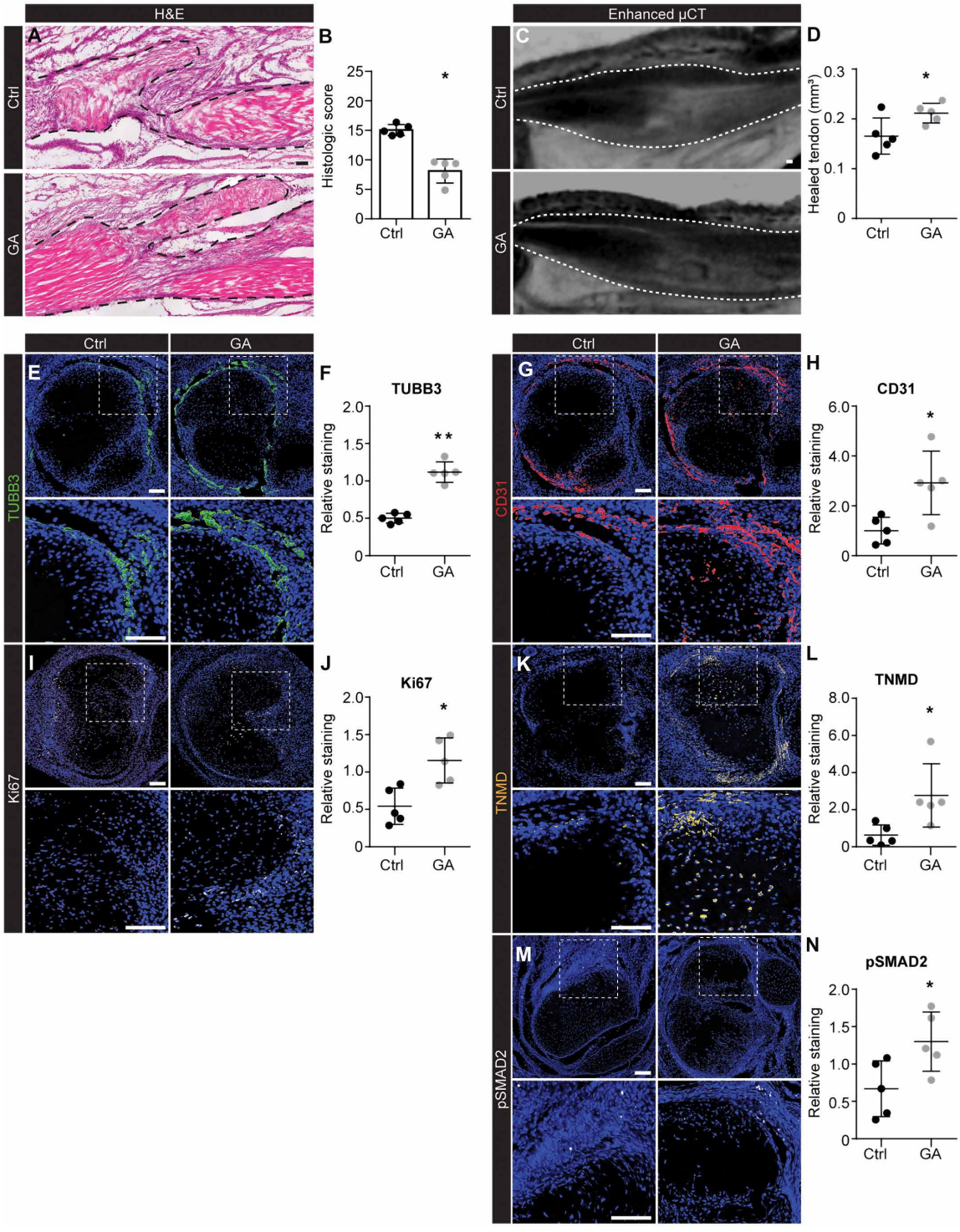

Fig. 8. TrkA agonism enhances tendon neurovascularization and repair. C57BL/6J 12-week-old (**A**) H&E staining performed on sagittal sections of the injury site. Dashed black lines indicate margins of tendon. (**B**) Histological score of healing (modified Movin's score), as assessed using H&E-stained sagittal sections. (**C**) Enhanced µCT imaging, shown in sagittal cross section. (**D**) µCT quantification of Achilles tendon volume within the injured area. (**E**) Assessment of tendon site innervation, using TUBB3 immunofluorescent staining of axial sections. (**F**) Quantification of (E). (**G**) Assessment of tendon site vascularization using CD31 immunofluorescent staining of axial sections. (**H**) Semiquantitative analysis of (G). (**I**) Assessment of tendon site proliferation using Ki67 immunofluorescent staining of axial sections. (**J**) Semiquantitative analysis of (I). (**K**) Assessment of TNMD immunofluorescent staining of axial sections. (**L**) Semiquantitative analysis of (K). (**M**) Assessment of pSmad2 immunofluorescent staining of axial sections. (**N**) Semiquantitative analysis of (M). Graphs show means ± 1 SD, and data points represent individual animal measurements. $*P < 0.05$; $**P < 0.01$ in comparison with control group. Two-tailed Student's *t* test. Scale bars, 100 µm. White dashed rectangles indicate areas of higher magnification. $n = 5$ mice per group.

higher histologic score reflective of poor healing (Fig. 6, C and D, and fig. S15). Whole-mount preparations of the uninjured and injured tendons with or without sural neurectomy were evaluated to assess tendon fiber organization 14 days after tendon injury (Fig. 6E). Analysis of collagen fiber orientation in SHG images showed that most of the collagen fibers were oriented at 90° in relation to the axial plane of the uninjured Achilles tendon (Fig. 6F). In injured animals, collagen fiber orientation was near 90° in the injured group, whereas the neurectomized injured animal showed marked collagen fiber disorganization with no consistent orientation (Fig. 6F). Nerve ingrowth and cell proliferation in the tendon injury site were assessed 14 days after tendon injury in injured or neurectomized injured animals (Fig. 6, G to J). Neurectomized animals had significantly less TUBB3 immunofluorescent staining ($P < 0.01$) and a significant decrease in Ki67 immunostaining ($P < 0.05$) (Fig. 6I). Sural neurectomy also caused a significant reduction of *Tppp3*$^+$ ($P < 0.01$) and a significant reduction of dual *Tppp3*$^+$*Scx*$^+$ cells at the injury site ($P < 0.05$) (Fig. 6J). To further understand the importance of innervation on TSPCs, fluorescence-activated cell sorting–isolated *Tppp3*$^+$ progenitors from the Achilles tendon (fig. S16) were cultured with neural conditioned medium (CM) derived from lumbar DRG cells (Fig. 6K). Neural CM induced significant proliferation of TSPCs after 24 hours ($P < 0.05$; Fig. 6L). Bulk RNA-seq was performed on TSPCs with or without neural CM stimulation (Fig. 6, K to O, and figs. S17 and S18). Of 25,588 total RNA transcripts, 113 were up-regulated and 77 were down-regulated with neural CM (fig. S17A and tables S7 and S8). Principal components analysis (PCA) showed a clear grouping of sample replicates (Fig. 6M). GO term and Kyoto Encyclopedia of Genes and Genomes (KEGG) pathway enrichment analysis among CM-treated TSPCs showed terms related to proliferation and angiogenesis, cell division and cytoskeleton organization, and signaling pathway activation, including TGFβ signaling (fig. S17, B and C). Last, module scores of curated activators and inhibitors gene sets confirmed significant enrichment in transcripts associated with proliferation ($P < 0.05$; Fig. 6N and fig. S18), TGFβ signaling pathway activation (Fig. 6O and fig. S18), and immune activation (fig. S18). In summary, bulk RNA-seq analysis revealed that neural CM stimulated TSPC cell proliferation and TGFβ signaling pathway activation.

Human tendon has innervation patterns that parallel those in mouse

The human relevance of sensory neuroregulation in tendon biology was next examined using available histologic tissues and transcriptomic data (Fig. 7). Histologic analysis of 20 human biceps tendons with varying degrees of tendiopathy revealed increasing TUBB3$^+$ staining of innervation within the tendon body and peritenon as the degree of tendinopathy increased (Fig. 7, A and B). In adjacent sections, more severe tendinopathy was also found to be associated with higher activation of TGFβ signaling, as indicated by elevated pSMAD2 immunostaining (Fig. 7C). A positive linear correlation was observed between the degree of tendinopathy (histologic score) and the volume of TUBB3-stained nerve fibers ($R^2 = 0.67$; Fig. 7D). An scRNA-seq database of cells derived from healthy and diseased human tendons (*40*) was used to examine cell clusters of tendon-resident cells (Fig. 7, E to I), which were identified by characteristic gene markers (Fig. 7, E and F). GO term and KEGG pathway enrichment analysis was performed across all cell clusters (Fig. 7, G and H), with diseased human tendon cells showing enrichment for terms such as angiogenesis, inflammatory response, axon guidance, and TGFβ signaling (Fig. 7, G and H, and tables S9 and S10). As in mouse tissues, predicted neural-to-tendon signaling interactions were performed using multitissue scRNA-seq data and NicheNet [1757 human DRG neurons obtained from (*41*)]. In parallel with the predicted neural-tendon interactome in the mouse, *TGFB3* was among growth and differentiation factors, axon guidance molecules, and neuropeptides predicted as neural-derived paracrine factors (Fig. 7I). This finding agrees with our human sensory neuron sequencing dataset in which *TGFB1* and *TGFB3* are expressed among *NTRK1*-expressing DRG neurons (*42*). In summary, human tendinopathy-associated innervation was highly associated with TGFβ signaling pathway activation.

A TrkA small-molecule partial agonist improves tendon repair

Having observed that genetic or surgical approaches to inhibiting NGF, TrkA signaling, or sensory nerves impeded tendon repair, we next sought to encourage tendon neoinnervation and repair by boosting TrkA activation. A small-molecule partial agonist of TrkA, gambogic amide [GA; 0.4 mg/kg, intraperitoneally (i.p.) daily over the repair period], was used to test the effect of stimulating TrkA in tendon injury. H&E-stained sagittal sections demonstrated improved overall organization and improved healing score among GA-treated tendon injuries (Fig. 8, A and B, and fig. S19). Enhanced μCT imaging confirmed these observations, showing a significant increase in healed tendon volume in the GA-treated group ($P < 0.05$; Fig. 8, C and D). As expected, TUBB3$^+$ peripheral nerve fibers showed a significant increase among GA-treated animals ($P < 0.01$; Fig. 8, E and F). Increased injury site innervation was accompanied by a significant increase in CD31$^+$ blood vessels in the GA-treated group ($P < 0.05$; Fig. 8, G and H). Improved healing metrics by TrkA partial agonism were accompanied by increases in cell proliferation and differentiation, as measured by Ki67 (Fig. 8, I and J) and TNMD immunostaining (Fig. 8, K and L). A significant increase in both Ki67 and TNMD immunostaining was observed around the tendon body among GA-treated mice ($P < 0.05$). Last, downstream effects of TrkA agonism on TGFβ signaling activation was assessed using pSMAD2 immunostaining, showing a significant increase in immunoreactivity with TrkA agonism when compared with injured animals treated with vehicle control ($P < 0.05$) (Fig. 8, M and N). Therefore, activation of TrkA signaling using a systemic small molecule has downstream effects of local tendon cell proliferation and differentiation, improving innervation, vascularization, metrics of tendon healing, and enhanced TGFβ signaling.

DISCUSSION

In this study, we demonstrated a crucial role for NGF-TrkA signaling in promoting sensory neurovascular response to positively regulating tendon healing. After injury, nerves sprout within the tendon injury site in parallel with TSPC and endothelial proliferation within the injured microenvironment. Rather than acting as a bystander in repair, tendon-associated nerves actively regulate TSPC proliferation and other niche factors to promote early tendon repair through activation of TGFβ signaling.

Our group reported the importance of TrkA in skeletal sensory nerve fibers in the regulation of long bone morphogenesis in primary and secondary ossification centers (*14*). Since then, evidence

that TrkA$^+$ sensory neurons regulate key aspects of skeletal morphogenesis and tissue repair continues to grow (*43*, *44*). TrkA$^+$ neurons are required for proper bone anabolic response to mechanical load (*45*), long bone stress fracture repair (*12*), cranial bone development and repair (*13*, *30*), and even abnormal bone formation in traumatic injury–associated heterotopic bone (*25*, *46*). These findings are consistent with a large body of literature regarding the role of peripheral neurons in regenerative processes across species (*47*, *48*). A common theme has thus emerged across contexts, in which TrkA$^+$ peripheral neurons provide proliferative signals in a paracrine fashion to skeletal progenitor cells and ECs during development and repair (*24*, *49*, *50*). In the current study, neural modulation of TSPC proliferation and differentiation was associated with alterations in TGFβ signaling, requiring activity of TrkA. In other experimental contexts, alternative signaling pathways have been implicated in neural-skeletal cross-talk, including FGF (*51*), vascular endothelial growth factor (VEGF) (*37*), hedgehog (*52*), and Wnt signaling (*53*) among others. Nevertheless, the therapeutic implications are clear, and stimulation of TrkA-expressing peripheral neurons has the potential for improving tendon healing.

Across four transcriptomic datasets in the present study, TGFβ signaling activation was implicated as downstream in nerve-tendon cross-talk. The exact secondary messengers that mediate this signaling are yet undefined. TGFβ ligands themselves, particularly TGFβ1 and β3 isoforms, were identified as potential neural regulators in mouse and human datasets. Alternatively, the neuropeptide substance P (SP) (present and highly expressed in TrkA$^+$ peripheral neurons) has been observed to increase TGFβ signaling in cultured tenocytes and could indirectly regulate tendon injury site TGFβ signaling (*54*, *55*). NGF itself has been shown to induce TGFβ expression, although, to our knowledge, this was not directly examined in tendon injury (*56*, *57*). Similar to the above neural regulation of tendon repair by TGFβ signaling, in our past report of the tendon-associated heterotopic bone, we observed that loss of innervation led to reduced TGFβ signaling among heterotopic ossification (HO)–associated progenitor cells (*25*, *46*). Mechanistically, it is unclear why tendon-associated nerves induce tendon repair in some contexts versus abnormal cartilage and bone formation in other contexts. We hypothesize that context-dependent factors, such as the degree and kinetics of inflammation within the injured tissues, the mechanotransduction changes relative to a complete or partial nature of tendon rupture (*58*), as well as ECM alignment (*59*) provide additional contributions toward determining proper tendon repair (*60*) versus heterotopic bone (*61*).

A high degree of neurovascular congruency exists during development, where peripheral nerves and blood vessels grow in tandem toward target tissues including ruptured tendons (*62*–*64*). This codependency is intuitive, because blood vessels transfer nutrients to axons, whereas peripheral nerves control vessel caliber (*65*). In our prior studies in bone morphogenesis and repair, inhibition of TrkA$^+$ peripheral sensory nerves led to substantial reductions in blood vessel numbers (*14*, *37*). In tendon-associated HO, our prior work showed that sciatic neurectomy led to a decrease in endothelial proliferation, reduction in a tip cell phenotype among ECs, reduced type H vessel formation, and a down-regulation of key transcriptional networks associated with angiogenesis (*37*). The similarity in EC phenotype between that and the present study is remarkable, despite distinct models and methods of neural inhibition. It is possible that deficits in principle neurotrophins (such as NGF) (*66*, *67*) and neuropeptides (calcitonin gene–related peptide and SP) (*68*, *69*) explain the EC phenotypes shared between these two studies, although other neural-derived proangiogenic factors, such as VEGFA and PDGFA, have also been implicated (*37*).

Several limitations to the current work deserve further discussion. First, the methods used to disrupt NGF-TrkA signaling pathway and induce hyperinnervation of the tendon repair site relied on systemic delivery. Although the effects are presumed to be primarily at the injury site, potential systemic effects of drug cannot be excluded. Second, our experimental paradigm is a surgical model of acute tendon injury. Far more common in clinical settings are chronic presentations of tendonitis or tendinopathy, which may (or may not) have similar neuroregulatory mechanisms. The contribution of mechanical loading in the context of sensory nerve disruption (surgical, chemical, or genetic) and its role in tendon healing and repair (*70*) are important aspects for future investigations. Third, other neuron types are established to express TrkA and respond to NGF, including sympathetic neurons (*71*, *72*). Future studies must examine the relative importance of sympathetic innervation in tendon repair, which may be distinct from sensory neurons. Fourth, neurovascular coupling is a clear component of our experimental models of tendon repair, as has also been shown in contexts of bone repair (*12*). Future experimental methods to "uncouple" these tissue repair responses may aid in the delineation of the relative contributions from each cell type. Last, as we are learning from recent single cell data of peripheral neurons (*32*), a large diversity of TrkA-expressing neurons exist, particularly in humans (*41*, *42*). Future work must identify the frequency, diversity, and transcriptional profile of neuronal subtypes that innervate deep somatic tissues such as tendon to help refine our understanding.

The present work identified the crucial role of TrkA$^+$ nerve fibers during tendon healing. Early ingrowth of NGF-responsive, TrkA$^+$ nerves regulate multiple cellular aspects of tendon repair, including mesenchymal, endothelial, and inflammatory cell behavior. In particular, *Tppp3*$^+$ TSPCs were dependent on innervation for their injury evoked proliferation. Last, our proof-of principle translational approach deserves further development, including testing additional small molecules to target TrkA$^+$ sensory neurons for improving tendon repair.

MATERIALS AND METHODS

Study design

The objective of the present study was to investigate the role of peripheral neurons in the process of tendon injury and repair. A murine Achilles tendon injury model was paired with histological and immunofluorescence imaging (table S11), SHG, μCT, detailed scRNA-seq, spatial-seq, and GO analysis to describe neurovascular response kinetics after tendon injury and the main molecular pathways involved in tendon healing. Transgenic mouse models (table S12) with conditional knockout of *Ngf*, chemical genetic knockin of TrkA mutant, or various reporter strains were used. Sural nerve transection was used to test the role of sensory neurons in tendon repair. Last, a small-molecule partial agonist of TrkA (GA) was tested as a therapeutic strategy for tendon healing.

Sample size was determined by a priori power analysis as explained in the "Statistical analyses" section. The end point of each experiment was predetermined and is noted in the text and figure legends (time points d7, d14, and d42). There were no inclusion/exclusion

criteria nor treatment of outliers in this study. All mice were randomly assigned to experimental groups; surgery and treatment were performed by a single operator; μCT, histological, and molecular measurements were performed in a blinded manner with respect to both genotype and treatment by at least two observers for independent replication. Sample numbers for all studies can be found in the figure legends. All procedures were performed under approval of the Johns Hopkins Animal Care and Use Committee (MO16M226 and MO19M366).

Statistical analysis

All data associated with this study are provided in data file S1. All analyses were performed by individuals blinded to genotype or treatment group. Quantitative data are expressed at means ± 1 SD, with $P < 0.05$ considered significant. The number of samples is indicated in figure legends. A Shapiro-Wilk test for normality was performed on all datasets. Homogeneity was confirmed by a comparison of variances test. Parametric data were analyzed using two-tailed Student's *t* test when two groups were being compared, or a one-way analysis of variance (ANOVA) was used when more than two groups were compared, followed by Tukey's multiple comparisons test. Nonparametric data were analyzed with a Mann-Whitney *U* test when two groups were being compared or a Kruskal-Wallis one-way analysis when more than two groups were compared. A priori sample size calculations were performed for experiments presented in Fig. 3 based on an anticipated effect size of at least 1.75, using our previously published data in adult $TrkA^{F592A}$ mice (*13*, *45*), such that five replicates per group and a two-sample *t* test would provide 80% power to detect effect sizes of at least 1.75 assuming a two-sided 0.05 level of significance.

Supplementary Materials

This PDF file includes:
Supplementary Materials and Methods
Figs. S1 to S19
Tables S1 to S12

Other Supplementary Material for this manuscript includes the following:
Data file S1
Movies S1 and S2
MDAR Reproducibility Checklist

REFERENCES AND NOTES

1. F. Wu, M. Nerlich, D. Docheva, Tendon injuries: Basic science and new repair proposals. *EFORT Open Rev.* **2**, 332–342 (2017).
2. N. L. Leong, J. L. Kator, T. L. Clemens, A. James, M. Enamoto-Iwamoto, J. Jiang, Tendon and ligament healing and current approaches to tendon and ligament regeneration. *J. Orthop. Res.* **38**, 7–12 (2020).
3. *The Burden of Musculoskeletal Diseases in the United States (BMUS)* (United States Bone and Joint Initiative, ed. 3).
4. E. Bussin, B. Cairns, T. Gerschman, M. Fredericson, J. Bovard, A. Scott, Topical diclofenac vs placebo for the treatment of chronic Achilles tendinopathy: A randomized controlled clinical trial. *PLOS One* **16**, e0247663 (2021).
5. D. P. Kuffler, Variables affecting the potential efficacy of PRP in providing chronic pain relief. *J. Pain Res.* **12**, 109–116 (2019).
6. C. Vannabouathong, M. Bhandari, A. Bedi, V. Khanna, P. Yung, V. Shetty, M. Khan, Nonoperative treatments for knee osteoarthritis: An evaluation of treatment characteristics and the intra-articular placebo effect: A systematic review. *JBJS Rev.* **6**, e5 (2018).
7. I. Andia, M. Abate, Platelet-rich plasma in the treatment of skeletal muscle injuries. *Expert Opin. Biol. Ther.* **15**, 987–999 (2015).
8. J. E. McAlister, Nonoperative management of the Achilles tendon insertion. *Clin. Podiatr. Med. Surg.* **39**, 477–487 (2022).
9. P. W. Ackermann, P. Salo, D. A. Hart, Tendon innervation. *Adv. Exp. Med. Biol.* **920**, 35–51 (2016).
10. P. W. Ackermann, S. L. Franklin, B. J. Dean, A. J. Carr, P. T. Salo, D. A. Hart, Neuronal pathways in tendon healing and tendinopathy - update. *Front. Biosci.* **19**, 1251–1278 (2014).
11. P. W. Ackermann, Neuronal regulation of tendon homoeostasis. *Int. J. Exp. Pathol.* **94**, 271–286 (2013).
12. Z. Li, C. A. Meyers, L. Chang, S. Lee, Z. Li, R. Tomlinson, A. Hoke, T. L. Clemens, A. W. James, Fracture repair requires TrkA signaling by skeletal sensory nerves. *J. Clin. Invest.* **129**, 5137–5150 (2019).
13. C. A. Meyers, S. Lee, T. Sono, J. Xu, S. Negri, Y. Tian, Y. Wang, Z. Li, S. Miller, L. Chang, Y. Gao, L. Minichiello, T. L. Clemens, A. W. James, A neurotrophic mechanism directs sensory nerve transit in cranial bone. *Cell Rep.* **31**, 107696 (2020).
14. R. E. Tomlinson, Z. Li, Q. Zhang, B. C. Goh, Z. Li, D. L. J. Thorek, L. Rajbhandari, T. M. Brushart, L. Minichiello, F. Zhou, A. Venkatesan, T. L. Clemens, NGF-TrkA signaling by sensory nerves coordinates the vascularization and ossification of developing endochondral bone. *Cell Rep.* **16**, 2723–2735 (2016).
15. A. S. Ahmed, J. Li, A. M. Abdul, M. Ahmed, C. G. Ostenson, P. T. Salo, C. Hewitt, D. A. Hart, P. W. Ackermann, Compromised neurotrophic and angiogenic regenerative capability during tendon healing in a rat model of type-II diabetes. *PLOS One* **12**, e0170748 (2017).
16. P. Gargiulo, P. J. Reynisson, B. Helgason, H. Kern, W. Mayr, P. Ingvarsson, T. Helgason, U. Carraro, Muscle, tendons, and bone: Structural changes during denervation and FES treatment. *Neurol. Res.* **33**, 750–758 (2011).
17. N. Maffulli, A. S. Irwin, M. G. Kenward, F. Smith, R. W. Porter, Achilles tendon rupture and sciatica: A possible correlation. *Br. J. Sports Med.* **32**, 174–177 (1998).
18. A. S. Ahmed, N. Schizas, J. Li, M. Ahmed, C. G. Östenson, P. Salo, C. Hewitt, D. A. Hart, P. W. Ackermann, Type 2 diabetes impairs tendon repair after injury in a rat model. *J. Appl. Physiol.* **113**, 1784–1791 (2012).
19. T. Mammoto, R. A. Seerattan, K. D. Paulson, C. A. Leonard, R. C. Bray, P. T. Salo, Nerve growth factor improves ligament healing. *J. Orthop. Res.* **26**, 957–964 (2008).
20. P. Burssens, A. Steyaert, R. Forsyth, E. J. van Ovost, Y. Depaepe, Y. De Paepe, R. Verdonk, Exogenously administered substance P and neutral endopeptidase inhibitors stimulate fibroblast proliferation, angiogenesis and collagen organization during Achilles tendon healing. *Foot Ankle Int.* **26**, 832–839 (2005).
21. O. Carlsson, N. Schizas, J. Li, P. W. Ackermann, Substance P injections enhance tissue proliferation and regulate sensory nerve ingrowth in rat tendon repair. *Scand. J. Med. Sci. Sports* **21**, 562–569 (2011).
22. A. E. Steyaert, P. J. Burssens, C. W. Vercruysse, G. G. Vanderstraeten, R. M. Verbeeck, The effects of substance P on the biomechanic properties of ruptured rat Achilles' tendon. *Arch. Phys. Med. Rehabil.* **87**, 254–258 (2006).
23. Q. Qin, S. Lee, N. Patel, K. Walden, M. Gomez-Salazar, B. Levi, A. W. James, Neurovascular coupling in bone regeneration. *Exp. Mol. Med.* **54**, 1844–1849 (2022).
24. J. Xu, Z. Li, R. J. Tower, S. Negri, Y. Wang, C. A. Meyers, T. Sono, Q. Qin, A. Lu, X. Xing, E. F. McCarthy, T. L. Clemens, A. W. James, NGF-p75 signaling coordinates skeletal cell migration during bone repair. *Sci. Adv.* **8**, eabl5716 (2022).
25. S. Lee, C. Hwang, S. Marini, R. J. Tower, Q. Qin, S. Negri, C. A. Pagani, Y. Sun, D. M. Stepien, M. Sorkin, C. A. Kubiak, N. D. Visser, C. A. Meyers, Y. Wang, H. A. Rasheed, J. Xu, S. Miller, A. K. Huber, L. Minichiello, P. S. Cederna, S. W. P. Kemp, T. L. Clemens, A. W. James, B. Levi, NGF-TrkA signaling dictates neural ingrowth and aberrant osteochondral differentiation after soft tissue trauma. *Nat. Commun.* **12**, 4939 (2021).
26. M. D. Kawaja, L. J. Smithson, J. Elliott, G. Trinh, A. M. Crotty, B. Michalski, M. Fahnestock, Nerve growth factor promoter activity revealed in mice expressing enhanced green fluorescent protein. *J. Comp. Neurol.* **519**, 2522–2545 (2011).
27. T. Movin, A. Gad, F. P. Reinholt, C. Rolf, Tendon pathology in long-standing achillodynia. Biopsy findings in 40 patients. *Acta Orthop. Scand.* **68**, 170–175 (1997).
28. G. Castaneda-Corral, J. M. Jimenez-Andrade, A. P. Bloom, R. N. Taylor, W. G. Mantyh, M. J. Kaczmarska, J. R. Ghilardi, P. W. Mantyh, The majority of myelinated and unmyelinated sensory nerve fibers that innervate bone express the tropomyosin receptor kinase A. *Neuroscience* **178**, 196–207 (2011).
29. X. Chen, H. Ye, R. Kuruvilla, N. Ramanan, K. W. Scangos, C. Zhang, N. M. Johnson, P. M. England, K. M. Shokat, D. D. Ginty, A chemical-genetic approach to studying neurotrophin signaling. *Neuron* **46**, 13–21 (2005).
30. R. J. Tower, Z. Li, Y. H. Cheng, X. W. Wang, L. Rajbhandari, Q. Zhang, S. Negri, C. R. Uytingco, A. Venkatesan, F. Q. Zhou, P. Cahan, A. W. James, T. L. Clemens, Spatial transcriptomics reveals a role for sensory nerves in preserving cranial suture patency through modulation of BMP/TGF-β signaling. *Proc. Natl. Acad. Sci. U.S.A.* **118**, (2021).
31. E. E. Govek, S. E. Newey, L. Van Aelst, The role of the Rho GTPases in neuronal development. *Genes Dev.* **19**, 1–49 (2005).
32. N. Sharma, K. Flaherty, K. Lezgiyeva, D. E. Wagner, A. M. Klein, D. D. Ginty, The emergence of transcriptional identity in somatosensory neurons. *Nature* **577**, 392–398 (2020).
33. R. Browaeys, W. Saelens, Y. Saeys, NicheNet: Modeling intercellular communication by linking ligands to target genes. *Nat. Methods* **17**, 159–162 (2020).

34. S. A. Fenwick, B. L. Hazleman, G. P. Riley, The vasculature and its role in the damaged and healing tendon. *Arthritis Res.* **4**, 252–260 (2002).
35. A. C. Noah, T. M. Li, L. M. Martinez, S. Wada, J. B. Swanson, N. P. Disser, K. B. Sugg, S. A. Rodeo, T. T. Lu, C. L. Mendias, Adaptive and innate immune cell responses in tendons and lymph nodes after tendon injury and repair. *J. Appl. Physiol.* **128**, 473–482 (2020).
36. S. Muscat, A. E. C. Nichols, E. Gira, A. E. Loiselle, CCR2 is expressed by tendon resident macrophage and T cells, while CCR2 deficiency impairs tendon healing via blunted involvement of tendon-resident and circulating monocytes/macrophages. *FASEB J.* **36**, e22607 (2022).
37. Q. Qin, M. Gomez-Salazar, M. Cherief, C. A. Pagani, S. Lee, C. Hwang, R. J. Tower, S. Onggo, Y. Sun, A. Piplani, Z. Li, S. Ramesh, T. L. Clemens, B. Levi, A. W. James, Neuron-to-vessel signaling is a required feature of aberrant stem cell commitment after soft tissue trauma. *Bone Res.* **10**, 43 (2022).
38. R. Blanco, H. Gerhardt, VEGF and notch in tip and stalk cell selection. *Cold Spring Harb. Perspect. Med.* **3**, a006569 (2013).
39. T. Harvey, S. Flamenco, C. M. Fan, A *Tppp3*$^+$*Pdgfra*$^+$ tendon stem cell population contributes to regeneration and reveals a shared role for PDGF signalling in regeneration and fibrosis. *Nat. Cell Biol.* **21**, 1490–1503 (2019).
40. A. R. Kendal, T. Layton, H. Al-Mossawi, L. Appleton, S. Dakin, R. Brown, C. Loizou, M. Rogers, R. Sharp, A. Carr, Multi-omic single cell analysis resolves novel stromal cell populations in healthy and diseased human tendon. *Sci. Rep.* **10**, 13939 (2020).
41. M. Q. Nguyen, L. J. von Buchholtz, A. N. Reker, N. J. Ryba, S. Davidson, Single-nucleus transcriptomic analysis of human dorsal root ganglion neurons. *eLife* **10**, (2021).
42. D. Tavares-Ferreira, S. Shiers, P. R. Ray, A. Wangzhou, V. Jeevakumar, I. Sankaranarayanan, A. M. Cervantes, J. C. Reese, A. Chamessian, B. A. Copits, P. M. Dougherty, R. W. Gereau 4th, M. D. Burton, G. Dussor, T. J. Price, Spatial transcriptomics of dorsal root ganglia identifies molecular signatures of human nociceptors. *Sci. Transl. Med.* **14**, eabj8186 (2022).
43. A. Leroux, B. Paiva Dos Santos, J. Leng, H. Oliveira, J. Amedee, Sensory neurons from dorsal root ganglia regulate endothelial cell function in extracellular matrix remodelling. *Cell Commun. Signal* **18**, 162 (2020).
44. N. Abeynayake, A. Arthur, S. Gronthos, Crosstalk between skeletal and neural tissues is critical for skeletal health. *Bone* **142**, 115645 (2021).
45. R. E. Tomlinson, Z. Li, Z. Li, L. Minichiello, R. C. Riddle, A. Venkatesan, T. L. Clemens, NGF-TrkA signaling in sensory nerves is required for skeletal adaptation to mechanical loads in mice. *Proc. Natl. Acad. Sci. U.S.A.* **114**, E3632–E3641 (2017).
46. M. Cherief, S. Negri, Q. Qin, C. A. Pagani, S. Lee, Y. P. Yang, T. L. Clemens, B. Levi, A. W. James, TrkA$^+$ neurons induce pathologic regeneration after soft tissue trauma. *Stem Cells Transl. Med.* **11**, 1165–1176 (2022).
47. M. G. Simoes, A. Bensimon-Brito, M. Fonseca, A. Farinho, F. Valerio, S. Sousa, N. Afonso, A. Kumar, A. Jacinto, Denervation impairs regeneration of amputated zebrafish fins. *BMC Dev. Biol.* **14**, 49 (2014).
48. M. Huet, Role of the nervous system during the regeneration of an arm in a starfish: Asterina gibbosa Penn. (Echinodermata, Asteriidae). *J. Embryol. Exp. Morphol.* **33**, 535–552 (1975).
49. Q. Q. Wan, W. P. Qin, Y. X. Ma, M. J. Shen, J. Li, Z. B. Zhang, J. H. Chen, F. R. Tay, L. N. Niu, K. Jiao, Crosstalk between bone and nerves within bone. *Adv. Sci.* **8**, 2003390 (2021).
50. K. Nakamura, F. Tan, Z. Li, C. J. Thiele, NGF activation of TrkA induces vascular endothelial growth factor expression via induction of hypoxia-inducible factor-1α. *Mol. Cell. Neurosci.* **46**, 498–506 (2011).
51. S. Li, N. Quarto, M. T. Longaker, Activation of FGF signaling mediates proliferative and osteogenic differences between neural crest derived frontal and mesoderm parietal derived bone. *PLOS ONE* **5**, e14033 (2010).
52. J. B. Regard, D. Malhotra, J. Gvozdenovic-Jeremic, M. Josey, M. Chen, L. S. Weinstein, J. Lu, E. M. Shore, F. S. Kaplan, Y. Yang, Activation of hedgehog signaling by loss of GNAS causes heterotopic ossification. *Nat. Med.* **19**, 1505–1512 (2013).
53. Y. Kishimoto, B. Ohkawara, T. Sakai, M. Ito, A. Masuda, N. Ishiguro, C. Shukunami, D. Docheva, K. Ohno, Wnt/β-catenin signaling suppresses expressions of Scx, Mkx, and Tnmd in tendon-derived cells. *PLOS ONE* **12**, e0182051 (2017).
54. N. Frara, P. W. Fisher, Y. Zhao, J. T. Tarr, M. Amin, S. N. Popoff, M. F. Barbe, Substance P increases CCN2 dependent on TGF-beta yet collagen type I via TGF-beta1 dependent and independent pathways in tenocytes. *Connect. Tissue Res.* **59**, 30–44 (2018).
55. G. Fong, L. J. Backman, H. Alfredson, A. Scott, P. Danielson, The effects of substance P and acetylcholine on human tenocyte proliferation converge mechanistically via TGF-β1. *PLOS ONE* **12**, e0174101 (2017).
56. Z. Shen, H. Tsao, S. LaRue, R. Liu, T. C. Kirkpatrick, L. C. Souza, A. Letra, R. M. Silva, Vascular endothelial growth factor and/or nerve growth factor treatment induces expression of dentinogenic, neuronal, and healing markers in stem cells of the apical papilla. *J. Endod.* **47**, 924–931 (2021).
57. S. J. Kim, K. Park, B. B. Rudkin, B. R. Dey, M. B. Sporn, A. B. Roberts, Nerve growth factor induces transcription of transforming growth factor-beta 1 through a specific promoter element in PC12 cells. *J. Biol. Chem.* **269**, 3739–3744 (1994).
58. A. K. Huber, N. Patel, C. A. Pagani, S. Marini, K. R. Padmanabhan, D. L. Matera, M. Said, C. Hwang, G. C. Hsu, A. A. Poli, A. L. Strong, N. D. Visser, J. A. Greenstein, R. Nelson, S. Li, M. T. Longaker, Y. Tang, S. J. Weiss, B. M. Baker, A. W. James, B. Levi, Immobilization after injury alters extracellular matrix and stem cell fate. *J. Clin. Invest.* **130**, 5444–5460 (2020).
59. C. A. Pagani, A. C. Bancroft, R. J. Tower, N. Livingston, Y. Sun, J. Y. Hong, R. N. Kent 3rd, A. L. Strong, J. H. Nunez, J. M. R. Medrano, N. Patel, B. A. Nanes, K. M. Dean, Z. Li, C. Ge, B. M. Baker, A. W. James, S. J. Weiss, R. T. Franceschi, B. Levi, Discoidin domain receptor 2 regulates aberrant mesenchymal lineage cell fate and matrix organization. *Sci. Adv.* **8**, eabq6152 (2022).
60. V. Arvind, A. H. Huang, Reparative and maladaptive inflammation in tendon healing. *Front. Bioeng. Biotechnol.* **9**, 719047 (2021).
61. M. Sorkin, A. K. Huber, C. Hwang, W. F. Carson 4th, R. Menon, J. Li, K. Vasquez, C. Pagani, N. Patel, S. Li, N. D. Visser, Y. Niknafs, S. Loder, M. Scola, D. Nycz, K. Gallagher, L. K. M. Cauley, J. Xu, A. W. James, S. Agarwal, S. Kunkel, Y. Mishina, B. Levi, Regulation of heterotopic ossification by monocytes in a mouse model of aberrant wound healing. *Nat. Commun.* **11**, 722 (2020).
62. Y. S. Mukouyama, D. Shin, S. Britsch, M. Taniguchi, D. J. Anderson, Sensory nerves determine the pattern of arterial differentiation and blood vessel branching in the skin. *Cell* **109**, 693–705 (2002).
63. P. W. Ackermann, M. Ahmed, A. Kreicbergs, Early nerve regeneration after Achilles tendon rupture — A prerequisite for healing? A study in the rat. *J. Orthop. Res.* **20**, 849–856 (2002).
64. L. Liu, R. Dana, J. Yin, Sensory neurons directly promote angiogenesis in response to inflammation via substance P signaling. *FASEB J.* **34**, 6229–6243 (2020).
65. P. Carmeliet, M. Tessier-Lavigne, Common mechanisms of nerve and blood vessel wiring. *Nature* **436**, 193–200 (2005).
66. M. Troullinaki, V. I. Alexaki, I. Mitroulis, A. Witt, A. Klotzsche-von Ameln, K. J. Chung, T. Chavakis, M. Economopoulou, Nerve growth factor regulates endothelial cell survival and pathological retinal angiogenesis. *J. Cell. Mol. Med.* **23**, 2362–2371 (2019).
67. S. K. Raychaudhuri, S. P. Raychaudhuri, H. Weltman, E. M. Farber, Effect of nerve growth factor on endothelial cell biology: Proliferation and adherence molecule expression on human dermal microvascular endothelial cells. *Arch. Dermatol. Res.* **293**, 291–295 (2001).
68. A. Haegerstrand, C. J. Dalsgaard, B. Jonzon, O. Larsson, J. Nilsson, Calcitonin gene-related peptide stimulates proliferation of human endothelial cells. *Proc. Natl. Acad. Sci. U.S.A.* **87**, 3299–3303 (1990).
69. P. I. Mapp, D. F. McWilliams, M. J. Turley, E. Hargin, D. A. Walsh, A role for the sensory neuropeptide calcitonin gene-related peptide in endothelial cell proliferation in vivo. *Br. J. Pharmacol.* **166**, 1261–1271 (2012).
70. E. Rio, D. Kidgell, G. L. Moseley, J. Gaida, S. Docking, C. Purdam, J. Cook, Tendon neuroplastic training: Changing the way we think about tendon rehabilitation: A narrative review. *Br. J. Sports Med.* **50**, 209–215 (2016).
71. X. Fang, L. Djouhri, S. McMullan, C. Berry, K. Okuse, S. G. Waxman, S. N. Lawson, trkA is expressed in nociceptive neurons and influences electrophysiological properties via Nav1.8 expression in rapidly conducting nociceptors. *J. Neurosci.* **25**, 4868–4878 (2005).
72. D. M. Holtzman, J. Kilbridge, Y. Li, E. T. Cunningham Jr., N. J. Lenn, D. O. Clary, L. F. Reichardt, W. C. Mobley, TrkA expression in the CNS: Evidence for the existence of several novel NGF-responsive CNS neurons. *J. Neurosci.* **15**, 1567–1576 (1995).

Acknowledgments

Funding: This work was supported by National Institutes of Health grants R21 DE027922, R01 DE031028, and R01 AR070773 to A.W.J.; National Institutes of Health grant R01 AR079171 to B.L.; Department of Defense grants USAMRAA W81XWH-18-1-0336, USAMRAA W81XWH-18-1-0121, USAMRAA W81XWH-20-1-0795, and USAMRAA W81XWH-20-1-0302 to A.W.J.; American Cancer Society grant RSG-18-027-01-CSM to A.W.J.; and the Maryland Stem Cell Research Foundation to A.W.J.. The content is solely the responsibility of the authors and does not necessarily represent the official views of the National Institute of Health or Department of Defense. **Author contributions:** M.C., J.X., Z.L., T.L.C., B.L., and A.W.J. conceptualized the project. M.C., J.X., Z.L., R.J.T., Q.Q., M.G.-S., J.-H.Y., S.L., S.N., and M.X. developed the methodology. M.C., J.X., Z.L., R.J.T., Q.Q., M.G.-S., J.-H.Y., S.L., S.N., M.X., and S.R. acquired and analyzed data. M.C., J.X., Z.L., S.R., J.-H.Y., S.L., S.N., and M.X. performed animal studies. R.J.T., S.R., and M.G.-S. performed computational analyses. T.P., A.R.K., and A.W.J. provided transcriptomic data. C.-M.F., T.L.C., and A.W.J. provided transgenic mice. B.L. and A.W.J. supervised the project and secured funding. M.C., J.X., Z.L., and A.W.J. were responsible for writing the original draft. T.P., C.-M.F., B.L., and A.W.J. handled review and editing of the

manuscript. **Competing interests:** A.W.J. is a paid consultant for Novadip and Lifesprout LLC for topics unrelated to the present work. This arrangement has been reviewed and approved by the Johns Hopkins University in accordance with its conflict of interest policies. All other authors declare that they have no competing interests. **Data and materials availability:** All data associated with this study are in the paper or Supplementary Materials. Transcriptomic data that support the findings of this study have been deposited in Gene Expression Omnibus (GEO) under SuperSeries GSE245179, GSE245097 for spatial-seq, GSE244921 for scRNA-seq, and GSE221035 for Bulk-seq. Human tendon transcriptomic dataset is available through Dryad (doi:10.5061/dryad.fxpnvx104). NGF-eGFP mice were graciously donated by the Kawaja laboratory through material transfer agreement with Queen's University at Kingston, Canada. $Ngf^{fl/fl}$ mice were donated by the Minichiello laboratory at the European Molecular Biology Laboratory (EMBL) through material transfer agreement with European EMBL, Germany. Tppp3-tdT-CreERT2;Scx-GFP mice were generously donated by the Fan laboratory for the research project (https://ventures.jhu.edu/technology-transfer/material-transfer-agreements/).

Submitted 31 January 2023
Resubmitted 30 June 2023
Accepted 29 November 2023
Published 20 December 2023
10.1126/scitranslmed.ade4619

Science Translational Medicine

TrkA-mediated sensory innervation of injured mouse tendon supports tendon sheath progenitor cell expansion and tendon repair

Masnsen Cherief, Jiajia Xu, Zhao Li, Robert J. Tower, Sowmya Ramesh, Qizhi Qin, Mario Gomez-Salazar, Ji-Hye Yea, Seungyong Lee, Stefano Negri, Mingxin Xu, Theodore Price, Adrian R. Kendal, Chen-Ming Fan, Thomas L. Clemens, Benjamin Levi, and Aaron W. James

Sci. Transl. Med. **15** (727), eade4619. DOI: 10.1126/scitranslmed.ade4619

Editor's summary

Tendons have peripheral nerve inputs for sensory feedback; however, the role of these nerves in tendon injury and repair remains unclear. Here, Cherief and colleagues demonstrated that an increase in peripheral nerve growth occurs after Achilles tendon injury in mice. Experimental blockade of nerve growth resulted in decreased tendon healing and reduced expansion of tendon sheath progenitor cells. Human tendon tissue imaging and transcriptomics corroborated the relationship between nerve growth and tendon healing. Last, activating the nerve growth factor receptor TrkA enhanced nerve responses to tendon injury, boosted progenitor cell expansion, and improved metrics of tendon repair. These findings implicate TrkA as a potential translational target to enhance tendon repair. —Molly Ogle